ktu
1922

KAUNAS UNIVERSITY OF TECHNOLOGY
FACULTY OF MATHEMATICS AND NATURE SCIENCES

Severina Paukštytė

DEVELOPMENT OF THE SLAB PHANTOM FOR THE MEASUREMENTS OF IRRADIATION DOSES IN SUPERFICIAL X-RAY THERAPY

Master's Final Degree Project

Supervisor

Lect. dr. Jurgita Laurikaitienė

KAUNAS, 2018

KAUNAS UNIVERSITY OF TECHNOLOGY
FACULTY MATHEMATICS AND NATURE SCIENCES

DEVELOPMENT OF THE SLAB PHANTOM FOR THE MEASUREMENTS OF IRRADIATION DOSES IN SUPERFICIAL X-RAY THERAPY

Master's Final Degree Project

Medical physics (code 621B92002)

Supervisor

Lect. dr. Jurgita Laurikaitienė

(date)

Reviewer

Prof. habil. dr. Arvaidas Galdikas

(date)

Project made by

Severina Paukštytė

(date)

KAUNAS, 2018

ktu
1922

KAUNAS UNIVERSITY OF TECHNOLOGY

(Faculty)

(Student's name, surname)

(Title and code of study programme)

'Development of the slab phantom for the

measurements of irradiation doses

in superficial X-ray therapy'

DECLARATION OF ACADEMIC INTEGRITY

20

Kaunas

I confirm that the final project of mine, Severina Paukštytė, on the topic 'Development of the slab phantom for the measurements of irradiation doses in superficial X-ray therapy' is written completely by myself; all the provided data and research results are correct and have been obtained honestly. None of the parts of this thesis have been plagiarised from any printed, Internet-based or otherwise recorded sources. All direct and indirect quotations from external resources are indicated in the list of references. No monetary funds (unless required by law) have been paid to anyone for any contribution to this project.

I fully and completely understand that any discovery of any manifestations/case/facts of dishonesty inevitably results in me incurring a penalty according to the procedure(s) effective at Kaunas University of Technology.

(name and surname filled in by hand)   *(signature)*

SUMMARY

Skin cancer is one of the most often registered cancer types in the world. In 2018 over 91 000 new cases of skin cancer have been reported (it contains 5.3% of all types of the cancer cases). Registered skin cancer cases in Lithuania contribute with 1 - 5 % to total number of all cancerous diseases. For this oncological disease treatment is usually used superficial X-ray therapy. Evaluation and reduction of if possible of radiation to the critical organs and normal tissues thus decreasing the risk of probability of secondary cancer is a very important issue controlling the disease process.

In order to asses irradiation doses superficial radiotherapy treatment was performed to irradiate a slab phantom, recreated from the real patient computed tomography images. 2D film dosimetry was used for the assessment of doses and evaluation of irradiation dose dependency on irradiation angle.

It was found that changing irradiation beam angle it is possible to reduce the dose to the critical organs depending their location. Performed investigation revealed that treatment beam angle is one of the optimization criteria ensuring also the quality during the superficial radiotherapy treatment of buccal skin cancer.

SANTRAUKA

Odos vėžys tai viena dažniausių pasitaikančių vėžio formų pasaulyje. 2018 metais jau užregistruota virš 91 000 naujų odos vėžio susirgimų ir tai sudaro 5.3% visų vėžio atvejų. Lietuvoje odos vėžys sudaro 1 - 5 % visų vėžinių susirgimų. Šiai onkologinei ligai gydyti yra taikoma trumpažidininė rentgeno terapija. Dėl galimybės kontroliuoti ligos eigą, labai svarbu įvertinti ir jeigu yra galimybė sumažinti apšvitos dozes sveikiems audiniams ir kritiniams organams, sumažinant antrinio vėžio rizikos tikimybę.

Šiame darbe trumpažidininės rentgeno terapijos apšvitos procedūra buvo atliekama naudojantis plokšteliniu fantomu, kuris buvo sukurtas pagal realaus paciento kompiuterinės tomografijos vaizdus. Apšvitos dozės buvo registruojamos 2D filmų dozimetrijos metodu, lyginant apšvitos dozių pasikeitimą priklausomai nuo apšvitos kampo kampo.

Nustatyta, kad keičiant apšvitos kampą galima sumažinti apšvitos dozę kritiniams organams, priklausomai nuo kritinių organų lokalizacijos. Atliktas tyrimas parodė, jog vienas iš būdų užtikrinti procedūros kokybę ir ją optimizuoti skruosto odos vėžio gydyme yra apšvitos kampo pasukimas

Content

Abbreviations

TSH – Thyroid Stimulating Hormone

OD – Optical Density;

FSD – Focus to Skin Distance;

IAEA – International Atomic Energy Agency;

ICRP - International Commission on Radiological Protection;

HN – Hygiene Standard (*liet. Higienos Norma*);

OAR – Organs At Risk;

TLD – Thermoluminescent Dosimeters;

QA – Quality Assurance;

NAS – National Academy of Sciences;

RPC – Radiation Protection Centre;

PMMA - Polymethyl Methacrylate;

MRI – Magnetic Resonance Imaging;

CT – Computed Tomography.

LAR – Lifetime Attribute Risk

BEIR – Biological Effects of Ionising Radiation

Figure content

Table content

Introduction

Skin is the largest tissue of the humans' body and it is a complex structure which consists of two major layers of epidermis and dermis and various types of cells. The outer layer of cells of the skin (~5 mm) is the area where the skin cancer might occur. Currently the field of interest in the skin cancer studies is the buccal (Eng. cheek) skin cancer due to its complex localization near highly differentiated critical organs and the possible cosmetic outcomes. Usually for buccal skin cancer the superficial radiation therapy is applied.

The main goal of radiotherapy is protection of normal tissues and critical organs, at the same time do not lowering the dose to the tumour. There is always a balance between a treatment and the possibility of complications [1]. Therefore, quality assurance in radiotherapy is one of the main issues ensuring efficiency of the treatment and patient's safety.

A dose measurement is one of methods, which helps to optimize irradiation procedures in diagnostic and radiotherapy fields. The buccal skin cancer in superficial radiotherapy is one of the intrigue issues evaluating irradiation doses during irradiation procedure for the normal tissues and critical organs. There are many different methods for the irradiation dose measurements. Evaluating effective dose it is possible to assess stochastic and deterministic effects. Usually it is done in diagnostic field for radiation protection purposes; however in radiotherapy evaluation of a lifetime risk is also useful for non-malignant diseases or non-targeted critical organs [2]. Irradiation doses measurements are not always possible during the irradiation procedure; in such kind of cases usually are used phantoms. Currently a lot of attention is paid on imitating irradiation procedures, recreating the phantoms from real size and shape patients, also imitating organs at risk and normal tissues. Therefore optimization of irradiation procedure and measurements of the irradiation doses is still in progress and real challenge for medical physicists. Due to economic and social factors in Lithuania not every institution could purchase the measurement equipment. Currently the problem is to assure the quality of the treatment procedure finding an effective method of irradiation doses measurements and evaluating for optimising treatment procedures, lowering the risk of secondary cancer.

Objective: to create and produce a slab phantom for irradiation doses registration and optimization of the superficial radiotherapy - treatment procedure for buccal skin cancer in superficial radiotherapy.

Tasks:

- To create and produce a prototype of 3D slab phantom recording configuration of anatomical regions;
- To measure absorbed doses in a slab phantom prototype using 2D films dosimetry and recreating the isodose distribution map.
- To recalculate effective doses from the measured absorbed doses for non-targeted critical organs and estimate the risks for the lifetime.

The MSc thesis were conducted in the Oncology Hospital of the Hospital of Lithuanian University of Health Sciences Kaunas Clinics.

1. Theoretical overview of head and neck skin cancer treatment and dosimetry

Superficial radiotherapy is a kilovoltage (maximum energy E_{max} = 50÷150 keV in the range of 50÷150 kV potential) X-ray therapy [3, 4].Superficial X-ray therapy is used for the treatment of cancers, which are at or close to the skin surface, due to the maximum prescribed dose absorption close to the surface of the body. The surface dose for superficial X-ray therapy photons is ~100 % of maximum, and the dose drops off rapidly in the deeper layers due to attenuation and scattering of the beam (fig. 1) [5]. For example it is known, that for 50 kVp beam the maximum of relative dose for 2 mm depth is 98%; 10 mm - 73% and 20 mm - 49% [6].
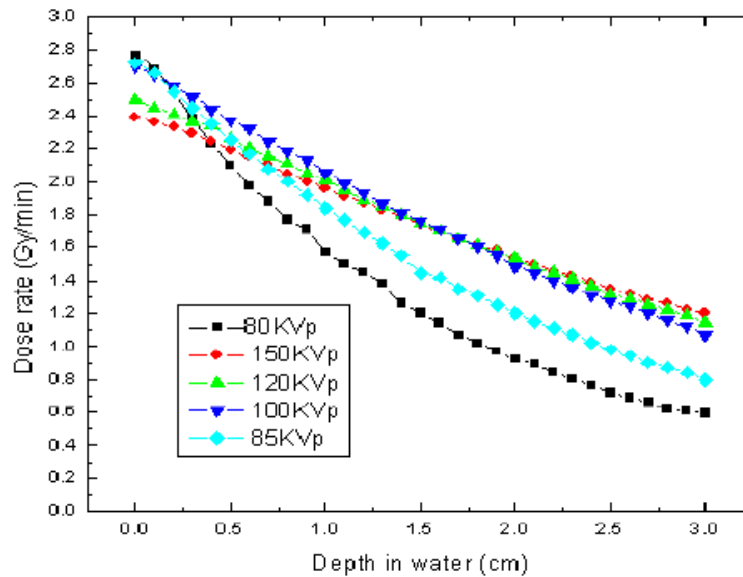
Figure 1. Dose depth characteristics of X-ray beams for 2.5cm applicator diameter [6]

Due to the characteristics of kilovoltage beams superficial X-ray therapy usually is used for the basal or squamous cell carcinomas of the skin, which are located near the surface and are not deeper than 5 mm (fig. 2) [5].
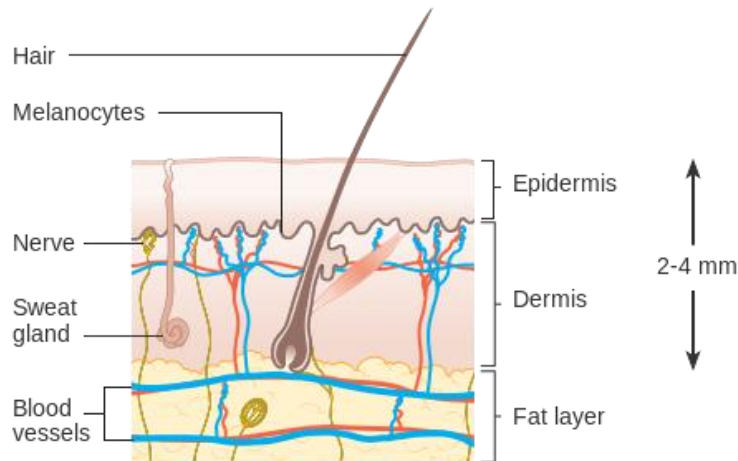
Figure 2. Skin surface [5]

It is known that the main purpose of superficial X-ray therapy is to deliver the maximum prescribed dose to the tumour, not exceeding the tolerance dose to the critical organs or healthy tissues, as an over dose may damage organs at risk (OAR), while lower dose may influence a quality of the treatment, making it less effective [6]. Therefore quality of the treatment procedure depends on optimisation of the radiation therapy procedure, for example, optimized radiation therapy technique appropriate choose of the applicator, energy of the beam, beam angle, application of the shielding to avoid early/ late side effects. [7, 8]. A lot of attention is paid to the head and neck tumours due to the healthy tissues and critical organs as salivary glands, thyroid, oesophagus, spinal cord, larynx and that at or close to the irradiation area.

1.2 Head – neck cancer treatment: dose prescription, critical organs, dosimetry

The range of energies used in superficial X-ray therapy is typically $E_{max} = 50 \div 150$ keV. The total prescribed dose depends on the localization of the tumour and its size. It might vary from 18 Gy to 66 Gy per whole treatment, while the dose per fraction and the treatment time might differ depending on characteristics of the tumour (table 1).

Table 1. Dose fractionation regimes - kilovoltage doses [9]

Prescribed dose	Fractions	Tumour identifications
18 Gy	1	Small tumour, cosmetic outcome not important
24 Gy	2 (five weeks apart)	Target < 5 cm, cosmetic outcome not important
35 Gy	5 (1 – 2 weeks)	Target < 2 cm
40.5 - 45 Gy	9 -10 (2 - 3 weeks)	Target size 5 - 6 cm
50 Gy	15 (3 weeks)	Target 4 - 6 cm
55 Gy	20 (4 weeks)	Target < 6 cm, OAR in direct beam pathway
60 - 66 Gy	30 - 33 (6 weeks)	Target > 6 cm, OAR in direct beam pathway

Prescribed dose depends on the localisation, size of the tumour and the outcome of the treatment. It is known that when near the tumour is localised the critical organs (thyroid, glandular tissues and etc.) usually the dose per fraction is lower (fig 3).

Figure 3. Soft tissue of head and neck area [10]

X-ray source applicator not always matches to the form of the tumour, due to this usually surrounding healthy tissues (e.g. skin, and etc.) are irradiated in higher dose. To optimize such kind of procedure sometimes is useful to use, for example, lead shielding [7]. Due to superficial radiotherapy delivering the maximum dose and the skin surface the healthy skin areas surrounding the tumour migh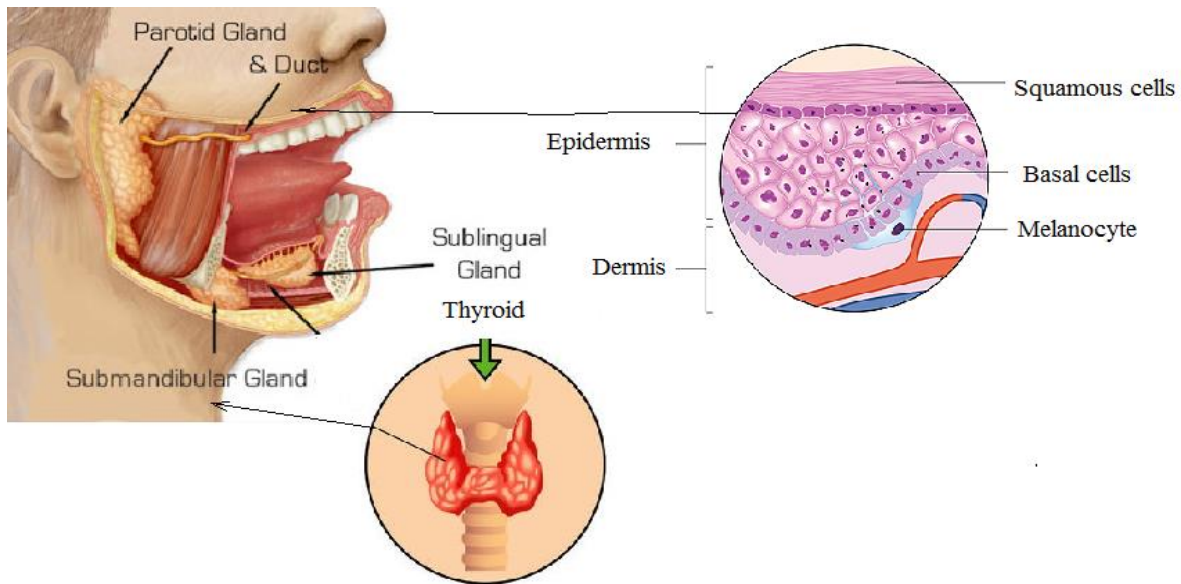t get irradiated with a high dose. The IAEA [11] presents that the risk of developing of non-melanomas' cancer increases linearly per Sievert (Sv) of effective dose.

In order to determine the possible risk for the critical organ, limitation to this organ should be taken into account. The radiation doses for the critical organs are still a question for discussion. The possible early and/or late effects observed during or after the treatment procedure depends on the delivered dose. For example, 1.8 – 2.2 Gy per fraction, 5 days a week for the salivary glands might cause redness, inflammation or infection; recovery period lasts approximately two weeks [12]; xerostomia (dry mouth syndrome) might be indicated in the first few days of the treatment with the doses of $2 \div 10$ Gy per fraction [13]; thyroid is considered to be a radiosensitive organ: it is assumed that a total dose of 30 Gy or more delivered to the thyroid during a treatment session results in a very high risk developing hypothyroidism, while other studies show that the TSH (Thyroid - Stimulating Hormone) hormonal levels of the thyroid significantly increases after receiving a total dose of 10 Gy during the treatment session [14].

In order to evaluate accuracy and the efficiency of a particular procedure, a lot of parameters have to be taken into account. These include the parameters of the used unit, clinical abilities, methodology of the irradiation procedure and quality assurance measurements.

1.3 Dosimetry and quality assurance

Quality assurance in Lithuania is controlled by the Health ministry along with the Radiation Protection Centre (*RSC – Radiacinės Saugos Centras*). The main requirements related with radiation protection, limits of irradiation dose, requirements for the equipment, standards of periodical measurements and etc. are determined and described in the Lithuanian Hygiene Standards [15]. The main Hygiene Norm for X-ray therapy is HN 95:2005 "Radiation protection and quality assurance in Radiotherapy" [16].

The main radiation therapy aim is to ensure quality of the treatment and safe dose delivery to the prescribed target volume and do not to exceed the irradiation tolerance levels to OAR [17]. Quality assurance (QA) program is necessary due to the high importance of the accurate dose delivery to the patient. According to Goran K. Svensson et. al. [1] it is observed dose change of target volume from 7 to 10 % and might lead to a change in a tumour control probability and an incidence of severe complications to surrounding tissues.

Scientific investigations showed that the main sources of errors occurring in radiation therapy such as tumour localization, patient immobilization, wrong field orientation or/and mistakes made in unit calibration process, calculations and equipment problems. Many of the errors, especially equipment – related calculations, can be avoided through daily checks/ measurements. For this reason, every radiation therapy facility must include a program addressed to the mechanical, radiation and electrical safety. Every program depends on the equipment of the facility. In general, quality assurance (QA) contains medically relevant recommendations about possible uncertainties in the dosimetrical field and mechanical alignment of the equipment [18].

All the QA procedures that assure the accuracy of radiotherapy can be characterized as it follows [17]:

- QA reduces all the possible uncertainties in dosimetry, equipment performance, treatment planning accuracy and its delivery therefore, giving an improvement to the precision of geometrical and dosimetrical treatment delivery. As a result it helps to control the tumour and reduces the risk of possible complications.

- QA not only reduces the possible accidents and errors that might occur during the procedure, causing a radiation accident but also it allows recognizing the problem before the damage is done, completing the treatment successfully.

- QA programs, protocols and documentation help to make a comparison between different radiation facilities assuring a uniform dosimetry. It also helps sharing all the experiences.

- QA helps to control the improving technologies by keeping the accuracy level high and constantly achieving the results.

The main concept is the QA of the radiotherapy equipment, which covers the voltage, electrical testing equipment, signals. Therefore, there are many protocols describing the QA requirements established by radiation safety facilities, such as IAEA (International Atomic Energy Agency) practice code TRS-398 which is applicable for Lithuanian radiation protection

standards [19]. Generally these programs include the acceptance tests for clinical applications, QA tests for new equipment, control test after significant repayments and a maintenance program that is recommended by the manufacturer.

1.4 Dosimetry methods and irradiation doses

Dosimetry is the way to measure and estimate ionizing radiation dose and to impose it to an individual case. It is important in radiation protection and is applied routinely thus to determine the appropriate dose delivered to the patient ensuring the safety and avoiding stochastic and deterministic effect on the body. The main task of dosimetry is to identify the absorbed radiation energy, i.e. dose in different environments and living organisms' tissues [20].

The measurement of the delivered dose is a complex estimation that depends on various factors and could not be easily solved so standardized solutions are introduced by the dosimetry communities such as ICRU (International Commission of Radiation Units); IAEA (International Atomic Energy Agency) and other medical physicists' societies. These communities introduce dosimetry protocols which give guidelines in determining the absorbed dose.

There are a few methods determining the absorbed dose according to International Atomic Energy Agencies practice code TRS-398 which includes chemical dosimetry, calorimetry and ionization dosimetry. Taking into account the primary standards of dosimetry these are the most accurate methods on describing the absorbed dose to water. There are various experimental approaches on estimating the absorbed dose. The absorbed dose is not an appropriate indicator to describe the biological effects to the human body. To calculate the biological effect out of absorbed dose tissue weighing factor and the radiation type effective dose could be calculated which represent the stochastic effect and risks of developing cancer [21].

Estimation of the dose is one of the factors based on the positioning of the patient and the delivered irradiation dose. Dose estimation includes the comparison of the prescribed dose and measured dose distribution. It is known that difference between the measured and prescribed doses should not be greater than 3% [22 - 24]. According to ICPR reaction of biological tissue is described by stochastic and deterministic effects. Based to ICRP 118 report [25] deterministic effects are the tissue reactions and these effects could not be predetermined during irradiation, but can be changed using various biological response modifiers, i.e. substances which that

modify immune responses. Deterministic effects usually have a threshold, which may be very low and may vary individually. Also, it is known that if the threshold was exceeded, then the severity of an effect increases depending on the increase of the absorbed dose [26]. ICRP Statement on tissue reactions and early and late effects of radiation in normal tissues and organs — threshold doses for tissue reactions in a radiation protection context [25]. Accordingly to this the effective dose could not be a measure of deterministic effects of the health, it is a measure of the severity of acute tissue damage that is happening as a quantity of absorbed dose [ICRP publication 103, 104 and 105 [27]. Stochastic effects usually occur incidentally can be compared to deterministic effects, which occur due to direct effect. Therefore for the stochastic effects it is important the probability of occurring, without dose threshold, but not the severity [28]. So there is no threshold and cancer risk increases in a so called linear-quadratic no threshold theory (LNT) with a dose. Though some studies [29] uses so called adaptive dose-response relationship: which claims that low doses are protective, while high doses are damaging [30]. Therefore the cancer risk increases with the dose, while the severity of effects does not and the patient will either develop cancer or they will not. To evaluate the possible cancer risk for the biological tissues and evaluation of effective doses for individual organs is needed. Especially it is very important in radiotherapy, where cancer risk in general is not suitable, because the patient already has developed a cancer. Effective dose is the dose of the ionizing radiation that is delivered to the tissue and is related to the incident reaction risks. These risks are described though cell mutation that is caused by DNA infringement, which usually is caused by small doses and it can be verified to each individual organ or tissues sensitivity level to the ionizing radiation. Knowing, that different tissues have a different sensitivity to the ionizing radiation, the International Commission on Radiological Protection has described the "effective dose" estimation as a purpose for radiation protection, involving the most sensitive organs and tissues by determining their weighing factors [31] (table 2).

Table 2. ICPR – 103 tissue weighing factors [21]

Tissue	Tissue weighing factor w_T	Sum of w_T values
Bone –marrow (red) lung, colon, breast, stomach, remainder tissues*	0.12	0.72
Gonads	0.08	0.08
Oesophagus, thyroid, bladder, liver	0.04	0.16
Bone surface, salivary glands, skin, brain	0.01	0.04
Total		1.00

*Adrenals, heart, extra thoracic (ET) region, lymphatic nodes, small intestine, gall bladder, muscle, oral mucosa, pancreas, spleen, thymus, kidneys, prostate (♂), uterus/cervix (♀).

The tissue weighing factors are revised values, which dependent on the risk of the cancer. Brain and salivary glands are the most recently included. Due to ICRP recommendations method of effective dose evaluation is generally used for radiation protection purposes for the general population irradiation evaluation and usually it is not applicable in radiotherapy field. However effective dose calculations for each organ individually, effective dose evaluation methodology in radiotherapy has a sense, especially assessing a lifetime risks for non-targeted critical organs [25]. Irradiation doses for the critical organs, like oesophagus, thyroid and salivary glands are in a big interest, due to their sensitivity to the ionising radiation. Due to the anatomical concern, it is recommended (if it is possible) to use some sort of lead shielding or change a geometry of irradiation procedure (angle of the beam, applicator, and etc.) for the thyroid and salivary glands. Regarding this issue many irradiation procedures are in interest, developing methods on keeping the dose to the critical organs as low as possible. The NAS (National Academy Of Sciences) [29] recommendations announces that the annual limit to the thyroid is 50 mSv. According to some studies salivary glands experience a 2 week healing process after receiving an effective dose of 18 – 22 mSv during a 5 day per week fractionation regime. [12]. Single dose of 20 mSv causes decrease of the saliva production and increases risk of secondary cancer. Other studies [30] show a possible dysfunction for the salivary glands regarding an effective dose: 1-5 mSv low, which usually do not show any specific signs, doses, 5 – 10 mSv medium doses, in some cases can be a dysfunction of flow rate, more rarely - swelling, 10 mSv and higher show a flow rate dysfunction

and sometimes swelling. Regarding the fractionation question, few fractions in high dose (15-40 Gy fraction, 2 – 3 times) is proven to result in cell loss and inflammation of the salivary glands however frequent fractions of small doses (2- 4 Gy of total 26 – 70 Gy) causes a parenchymal loss and flow rate reduction due to repeatable damage to the same area [31]. Accordingly to this the effective doses evaluation during the superficial radiotherapy treating the skin of facial area is still of a great interest, regarding to the possible lesions, the risk of the secondary cancer and/or permanent damage to the gland function. Keith Baverstock's [27] study explaining how much radiation is harmful for the human body. The study described the typically during one single procedure the effective dose being an average of 10 to 20 mSv to the whole body. It has been proven that an annual intake of 100 mSv of effective dose evidently increases the risk of the cancer [28].

The dose limits and the possible risks are determined though dosimetrical measurements. The measurements and dose evaluation are carried out using particular dosimetrical equipment. Different methods allow the evaluation of the doses to be more accurate and reasonable [20].

1.6 Dosimetrical methods and tools

The measurement of the delivered dose is a complex process which depends on various factors and could not be easily solved. Standardized solutions, like dosimetry protocols, environmental conditions and the tools that are used to measure the prescribed dose, are introduced by ICRU (International Commission of Radiation Units); IAEA (International Atomic Energy Agency) and other medical physicists' societies [33].

There are a few methods determining the absorbed dose according to International Atomic Energy Agencies practice code TRS-398 [19] which includes chemical dosimetry, colorimetric and ionization dosimetry.

Therefore dosimetrical verification before the patient's treatment is an important "key" ensuring an accurate and precise treatment delivery in radiotherapy. So ionization chambers, TLDs and films dosimetry are the main "tools" mostly used in radiotherapy for dosimetry purposes.

1.6.1 Dosimeters for absorbed dose evaluation

In application on medical dose measurements a number of important factors are presented selecting an appropriate dosimeter for the measurements of the dose [33]. The most important is accuracy (73% in the range of the measurements from a few miligrays to 10 Gy), the limit of detection, energy absorption range, the energy dependence in different radiation energies, easy usage. By following the guidance the selection is limited to few reliable tools.

The most frequently used "tool" for absolute dosimetry are ionization chambers, which are used for detecting kilovoltage or megavoltage photon beams [19]. Dosimeters that are widely known in the medical field and described by IAEA are thermo - luminescent dosimeters TLD and GAFchromic films [34]. It states the precision of the TLD of ±3% as it is announced by the American Radiologic Physics Centre (RPC) [1]. The TLDs could be described as a tool for the dose verification in certain depths by combining TLD matrixes and evaluating the dose distribution to each dosimeter [33]. GAFchromic films are also introduced to dosimetry as a tool for absorbed dose estimation in certain depths. It introduces to a quite high spatial resolution in a wide region of radiation qualities.

Ionization chambers

According to IAEA TRS-398 practice code [19] the ionization chamber standard introduce to a graphite cavity chamber that provides accuracy by knowing the chamber volume that is designed to fulfil the Bragg – Gray detector requirements as far as possible. The ionization chamber should be placed in a phantom at a certain depth and the absorbed dose to water is determined at a reference point given by a mean specific energy to the cavity filled with air [34].

The ionization dosimetry includes equipment an ionization chamber with a cable that is electrically fitted to the chamber, a measuring device such as an electrometer that is calibrated and waterproof phantoms that is fitted for the ionization chamber with a waterproof sleeve.

The ionization chamber is the most commonly used dosimetry device including daily, weekly or monthly check as it is easy to use and is enough high. In superficial radiotherapy the chamber should be designed regarding kilovoltage energy X-rays. The chamber window should be thick enough to allow the secondary electron spectrum build–up. This way the electrons will be prevented from entering the chamber. The X-ray voltage being 50 kV or above foils or other materials should be used on the window to ensure the full build-up. The window might be thickened with plastics – polyethylene (for 80 kV 100µm), PMMA (80kV – 85 µm), Mylar (80 kV – 75 µm) [19].

Although it is a simple solution in routine check and gives a wide range of radiation energy response it has its own drawbacks, thus not providing the spatial resolution as it is positioned at a certain point.

Thermo - luminescence dosimeters (TLD)

Thermo luminescence dosimetry is based upon the ability of imperfect crystals to absorb and store the energy of ionizing radiation, which upon heating is re-emitted in the form of electromagnetic radiation, mainly in the visible wavelength. The light emitted is then detected by a photomultiplier (PM) and correlated to the absorbed dose received by the TL material [35].

There is a variety of thermo luminescent dosimeters and TL materials available such as CaSO4:Dy, LiF:Mg,Ti, LiF:Mg,Cu,P, 7LiF:Mg,Cu,P and more in all kinds of geometric shapes (chips or pellets, single crystals, rods, powders, ribbons and gel), which are produced from materials close to biological tissue.

TLD's are presented as a convenient tool for ionizing radiation dosimetry using solid state phantoms determining the absorbed dose in a certain depth. It has been gaining popularity in determining the dose spatial resolution. Researchers such as M. Zelikman *et. al*. had done experiment involving a TLD matrix in phantom (fig. 4) by drilling holes for a TLD input [36]. The amount of the holes depend on the body area that is in interest and the distance between the areas depend on a researchers wish to determine the distribution.

Figure 4. Models with TLD matrix [37]

TLD's are described as a precise tool according to American RPC (Radiation Protection Centre) [11]. Although it is a tool that it is easy to use, TLD have and its limitations: the readout process could not be achieved at a real time also it is energy dependent [38]. The response is dependent on the ionizing radiation energy (fig. 5). Thus if the TLD is chosen in an experiment it must be calibrated in the same conditions as the experiment would be carried out.
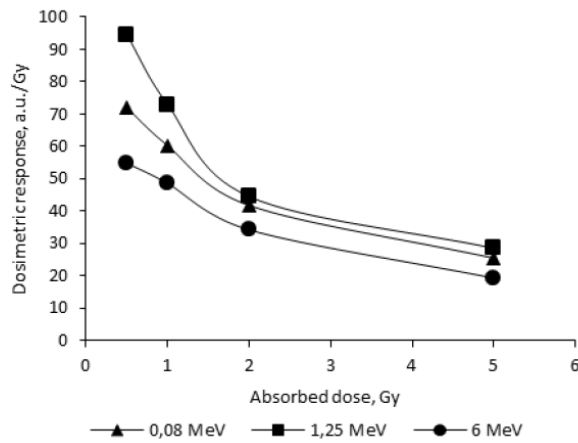

Fig. 5. The response of absorbed dose per 1 Gy in different radiation energies [38]

GAFchromic films

GAFchromic films are developed for measuring absorbed doses and depending on the manufacturer and film type can be sensitive and various energy ranges. Although the dynamic range is from 0.1 to 40 Gy, GAFchromic films perform best when the dose range varies from 0.2 to 10 Gy making it acceptable for many applications. Figure 6 shows the structure of a GAFchromic film. It has three layers. The active layer is placed between two polyester layers. Usually the active layer is a few micrometres thick and it varies depending on the manufacturer, for example, the HD-810 has Active layer of 7 μm thick and a polyester base of 99 μm, while MD – 55 -1 and MD – 55 – 2 had the active layer of 15 μm and a polyester base of 67 μm [39].

Polyester Overlaminate - 50 microns

Adhesive Layer - 25 microns

Topcoat - 5 microns

Active Layer - 30 microns

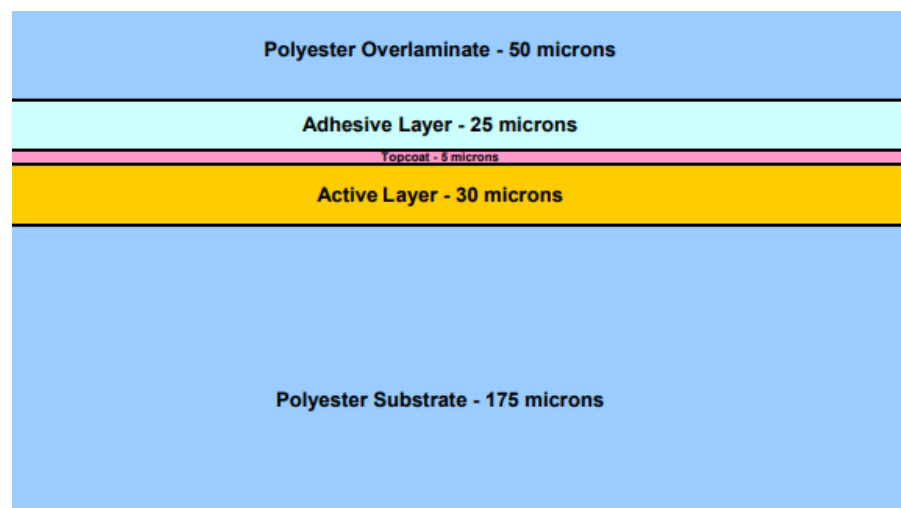**Polyester Substrate - 175 microns**

Figure 6. Structure of dosimetry GafChromic EBT2 film [39]

McLaughlin et al. [40] studied the GAFchromic films as a solid-state polymer where the films turn their colour into blue, depending on the delivered radiation dose (higher dose, more blue the film). The changes in polymer (poly-conjugated polymer chains) lead to colour changes [41].

GAFchromic films have its advantages of not being energy dependent. Also it can be stable at environmental temperatures up to 60°C and has insignificant dependency on the humidity. Gafchromic films can be handled in a lighted room for short periods of time with no visible effects [40].

After the exposure change in colour can should set and be more accurately determined in the following 24-48 hours. The colour change is usually measured at a narrow point in spectral wavelength band using a densitometer, spectrophotometer or image analysing systems. It shows the optical density *OD*, which is described through a decimal logarithm: the ratio of the transmitted light through the film *I* to the incident light on the film I_0 (1) [42]:

$$OD = log_{10}\left(\frac{I}{I_0}\right) \quad (1)$$

As it is seen ionization chambers, TLDs and films dosimetry "tools" are enough accurate, easy to use in radiotherapy for dosimetry purposes, but simulating the "real" situations in radiotherapy usually are used so called phantoms for radiation therapy QA.

1.6.2 Phantom dosimetry

Following the TRS-398 protocol [19] phantoms may vary by their size and the material type that they are made from. The main thing is to assure that it was equivalent to the human body. It refers that human has 70% of water in the body mass so the absorbed dose should be calculated regarding absorption to water. Depending on the beam energy a variety of requirements are made for phantoms: size, thickness, density, type of material (poly-methyl methacrylate (PMMA), water, and etc.).

Earlier made investigations gave the ability to create various types of phantoms that are water equivalent by comparing the measurement with a known depth in water [42, 43, 44]. Today usually two main types of phantoms are used in daily routine: water phantoms and solid state phantoms.

Water phantoms

Water phantoms are suitable for determining the absorbed dose for photon beams. Water phantoms give the ability to measure the ionizing radiation dose in a certain depths as it represents the human body during the treatment procedure [19].

According to IAEA TRS-398 [19] water phantoms are the most suitable for radiation dose measurements. The phantom is created for absolute dose measurements for high energy photons and electron beams. Usually it is cube shape and has requirements for the sleeve where the dosimeter should be placed, made out of thin plastic. The size of the phantom varies depending on the radiation field size. In size the phantom size must exceed at least 5 cm to all sides regarding the field size and exceed at least 5 g/cm^2 of the maximum measurement depth [19].

The newest motorized water phantoms allows to change remotely the depth and the positioning of an individual dosimeter (fig. 7)

Figure 7. Motorized water phantom for absolute dosimetry measurements [43]

Solid state phantoms

These phantoms are made out of material that is water equivalent, like plastic, PMMA, solid water, virtual water, plastic water. The absorbed dose using these phantoms should always be referred to water. The material should have similar scatter and absorption properties as water phantoms. The size, height, ionization camera sleeve has the same requirements as a water phantom. Solid state phantoms gain a lot of popularity lately due to the easy usage.

According to TRS-398 protocols [19] plastic phantoms cause uncertainties of measurements due to the density variations between different phantom manufacturers. The absorbed dose should be referred to absorbed dose to water so the requirement for plastic phantom is to give a nominal value for the plastic type that is the mean thickness and density. Solid state phantoms are used in routine checks quality assurance and calibration.

Currently the variety of solid state phantoms is really large, but the mostly used is the PMMA phantom. Two main types of solid state phantoms: 1) a standard phantom is a PMMA block (fig. 8 – a) which contains a cavity for the ionization chamber. Depending on the measurement type the depth can vary and there are some sort of adapters, which allows to avoid the air gaps nearby the chamber ensuring the effectiveness of the measurements [18, 45]; 2) using PMMA plate phantoms is possible to vary thickness of the plates, which can be built into a block (fig. 8 – b), which also have a cavity for an ionization chamber; this type of the phantom is more suitable to use for different types of detector measurements in certain depths, also it is easy to place a GAFchromic film or to place a TLD matrix between the plates. Both standard and plate phantoms are IAEA TRS-398 approved and can be used for quality assurance and calibration [19].
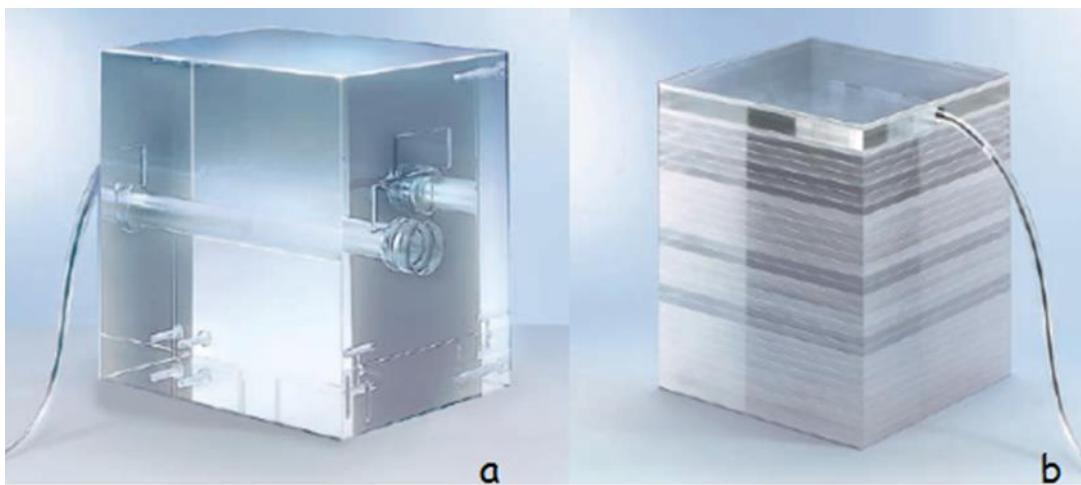

Figure 8. PMMA phantoms: a – standard PMMA phantom; b – PMMA plate phantom [43]

Voxel phantoms

Standard water and solid state phantoms is still successfully used till now. However their have certain limitations (uncertainties due to their state and form), so today it is possible to use more accurate methods, simulating real size organs and body parts of human body, using such kind of phantoms in dosimetry field for irradiation dose verification and optimization of radiotherapy procedures. Such kind of the phantoms could be made from different types of material, also could be like water or solid state phantoms.

According to ICRP – 103 [44] the main point of radiotherapy is to lower the dose to the critical organs and most sensitive healthy tissues. In this case, voxel human water phantoms are making a progress imitating human body parts and helping to determine ionizing radiation effects. Yoshitomi *et. al.* [45] studied the effects on the lens of the human eye. The idea was to create a cylindrical slab phantom and a human head phantom for determination the backscatter effect more properly. Studies show the changes of the calibration factor and represented the scatter effect is 10 % higher in the human head phantom then is cylinder due to the differences of the volume using photon beams with 80 keV energy.

Solid state human phantoms are popular due to easy usage. Solid state voxel phantoms introduce the simulation of the human body. It is based on the magnetic resonance imaging (MRI) and computed tomography (CT) [46]. These devices generate images of the human body and three dimensional body parts and organs may be simulated into a phantom. The images are transformed into volumetric pixel format and are recreated into a digital form in 3D as shown in figure 9.
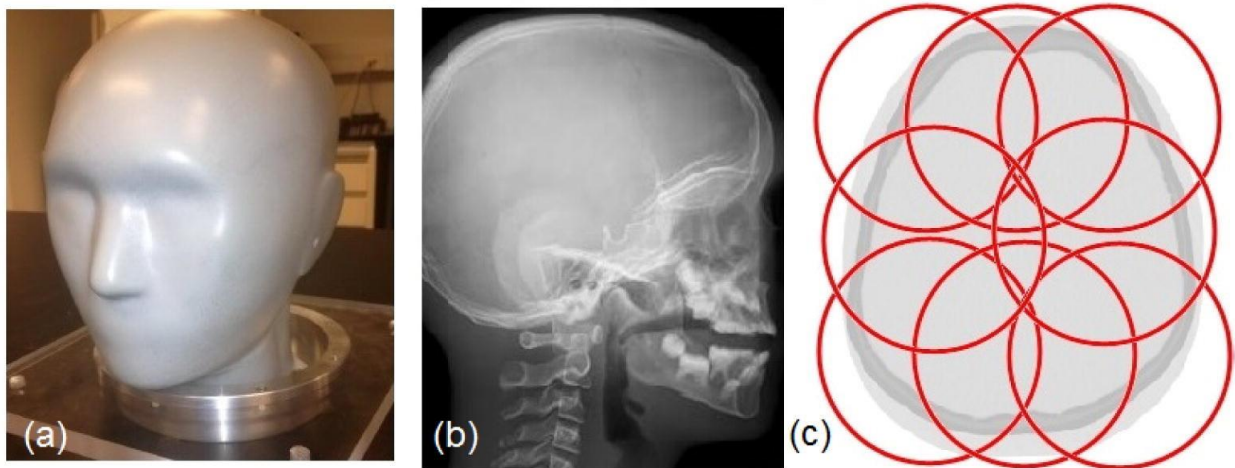

Figure 9. Solid state human phantom: (a) Voxel head phantom; (b) X-ray radiograph with anatomical detail (c) arrangement of simulation into a phantom [44]

V. Giacomettia et al. [46] study is shown in Fig X. this study represents the results of the measurements made with a phantom, which was made out of tissue equivalent material, depending on the density, that represents a paediatric case of 5 year old kids and the possible effects of the body during the proton therapy. The voxel phantom recreation is made by adding X-ray imaging of anatomical structures and CT scans for the size recreation.

Another type of the voxel phantoms are so called *voxel slab phantoms*, which are superior to the standard voxel phantoms, due to their ability to locate different types of measurement devices, so could be measured and get a better understanding about the dose and/ or dose distribution during irradiation procedure and about possible physical processes, which occur in the phantom. Voxel slab phantoms also could be used in both forms: water and solid state. Solid state ones are more popular due to easier usage in daily routine. The main advantage is the accurate location of the critical organs that need to be examined by having the ability to recreate the model of the human body and making slices of it as thick as it is needed [47]. Plated slab phantom are suitable in dosimetry using low energies (10 – 100 kV) thus making it suitable for superficial radiotherapy. Depending on the dosimeter chosen and its placement between the slabs it has an ability to show the experimental spatial distribution of the dose delivered to a certain body part making it suitable in planning each procedure (fig 10).
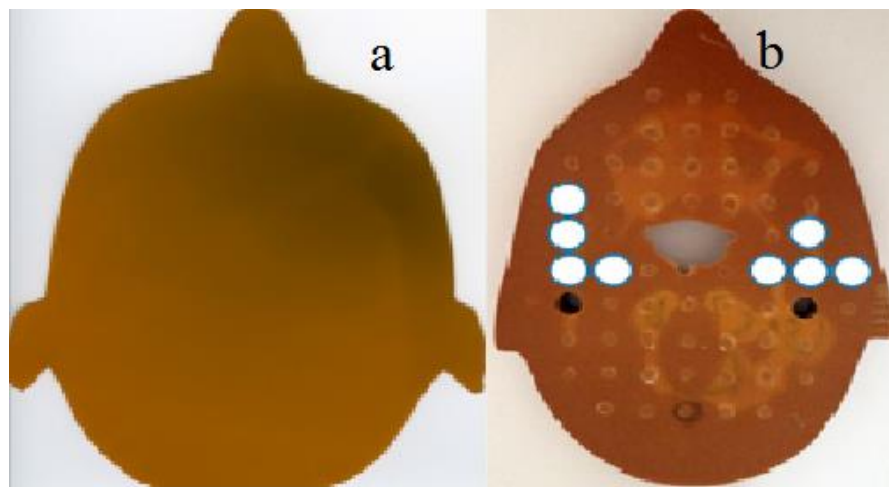

Figure 10. Plated – slab phantom of head, showing spatial distribution of dose; a – using GAFchromic films; b – using TLDs [48]

Figure 10 represent the plated slab phantoms might provide a lot of information thus leading to a better radiation protection system by examining the prescribed treatment on the type of phantom. It may help adjusting the positioning and the dose used for each planned procedure and showing the possible risks of the critical organs [48].

Using voxel phantoms helps providing reliable information and allowing planning a suitable diagnostic or treatment circumstances to an individual patient. It is especially helpful in superficial radiotherapy, due to the easier positioning of the dosimeter in each slab giving the ability to show the spatial distribution of the dose in certain body parts. This leads us to optimized procedure of radiotherapy and the irradiation dose during procedure.

1.9 Summary of theoretical overview

Worldwide there are a lot of studies and methods developed in order to determine the dose delivered to the critical organs. When it comes to superficial radiotherapy as a therapy for the skin cancer using low irradiation voltages (50÷150 kV) there is not enough informative data about the possible stochastic and deterministic effects. Easily manageable methods should be introduced in order to collect information about the possible risks to the OAR.

Phantom dosimetry is one of the convenient methods for the accurate dose measurements could be. Real size human body 3D models of the phantoms imitating could be more accurate and more realistic. In superficial radiotherapy the biggest concern is the head and neck area, where the critical organs are distributed throughout the area where it is hard to protect.

For the measurements of the irradiation doses the slab phantom could be used registering irradiation doses TLD or GAFchromic film dosimetry for the critical organs and normal tissues. It is a new method which could be useful for optimization of procedures of superficial radiotherapy assessing possible risks.

2. Methodology

Absorbed and effective doses of organs at risk were evaluated using poly-methyl methacrylate (PMMA) slab phantom reconstructed from the real patient computed tomography (CT) scans, imitating head and neck area for skin cancer (bucca) irradiation procedure.

2.1 3D imaging and reconstruction of the head and neck area

The first step of creating a slab phantom was to recreate a real standard patient from 3D computed tomography scans. The phantom is an imitation of the real life sized human body parts. The bucca skin cancer case was imitated in this research work using created PMMA slab phantom. Comparing the skeletal differences between standard males and females it is known, that the bone structure differs. Males have a thicker bone mass and the mandibular is more angular than females, but all the soft tissues or critical organs remains in the same position [49].

The next step requires a program 3D slicer to transform the CT scan of the human body into a 3D digital form, thus leading to a model of the investigated body part. The program uploads *.dicom* images that may be visualized in a 3 – dimensional form. It gives the ability to manipulate the whole image by removing/adding structures (bones, soft tissue) and slicing it in different projections. Usually this program is used for 3D printers (fig. 10).
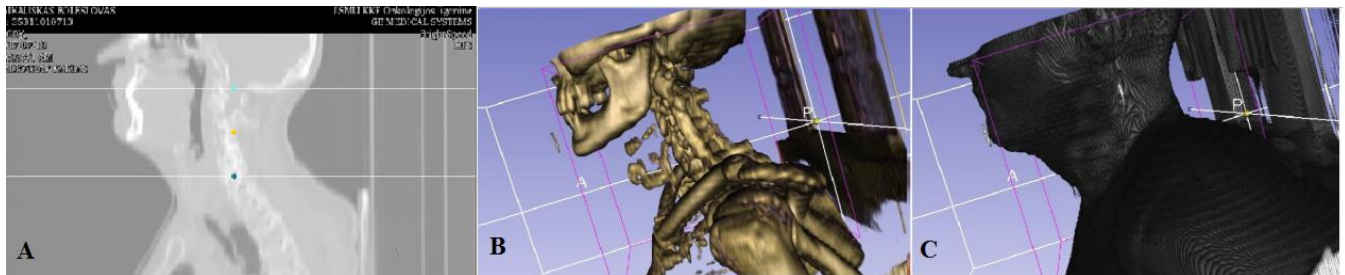
Figure 11. Chosen area of interest – head-neck area; A – CT scan; B – bone structure; C - soft tissue structure

The area of the head and neck is interesting due to its organs at risk, which is usually nearby irradiated area. The slab phantom was made from PMMA, recreating from CT scans an accurate location of the critical organs: three largest salivary glands (parotid, submandibular, sublingual), oesophagus and thyroid (fig. 11). In order to recreate bucca skin cancer case, were

chosen region of head and neck from C1 to C6 vertebrae (8 cm) and divided into slabs of 2 cm (in total: 4 slabs). Figure 12 shows possible locations of critical organs in slabs in compare with CT scan images respectively.
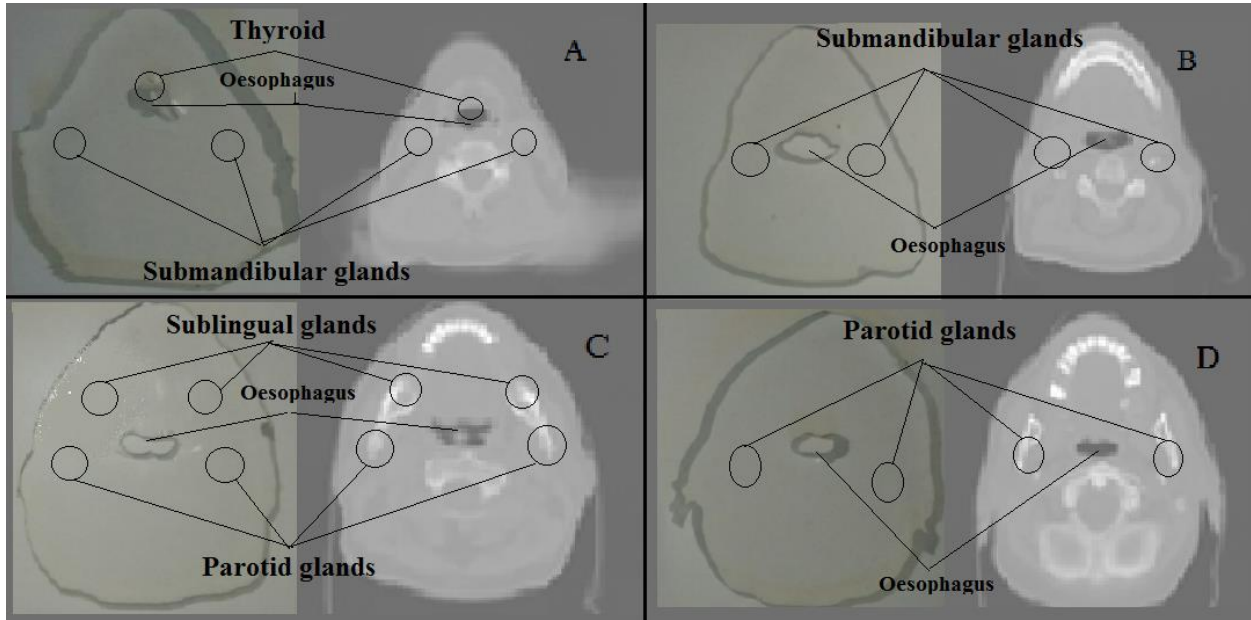

Figure 12. The slices of the head-neck area; A - neck, B, C, D – lower mandibular

After the formatting the head and neck area of interest using 3D slicer the 3D image in *.dll* format is uploaded to Blender program. Blender applies a smoothening function on the slices defined from the 3D slicer. This is done in order to approach the smoothness of chosen head and neck region, as using 3D slicer is impossible to correct the lines and edges of the recreated images (fig. 13).
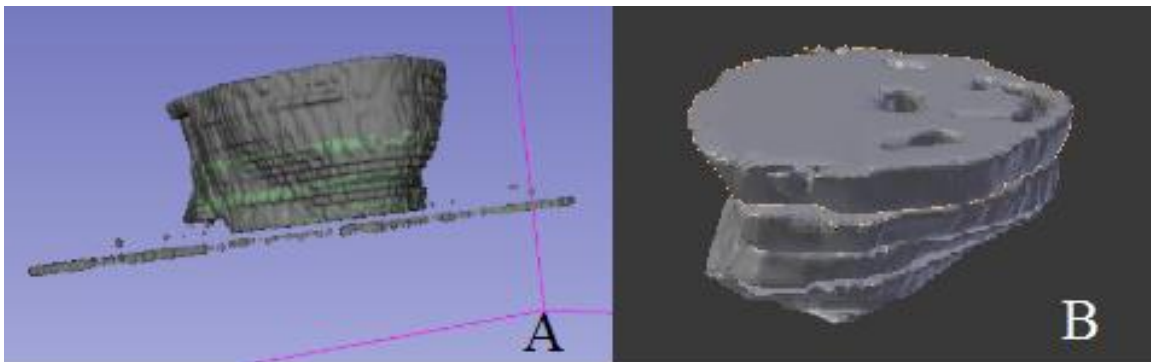

Figure 13. Comparison of the head-neck area; A – 3D slicer, B - Blender

The finished reconstructed slab phantom prototype is shown in figure 12 - B As it is clearly seen, the edges here are smoothened recreating the lower part of mandibular. Blender program allows to get the prototype that will be received/created in reality.

2.2 Production of slab phantom

In order to reconstruct the 3D model slab phantom prototype to a PMMA slab phantom, PMMA plates has to be cut as mentioned before into 2 cm thickness slabs. Abrasive water jet cutting technology was used for it. The technology has limitations because the form of the slab could only be cut perpendicular to the surface. For this reason the 3D form slices has to be remodelled into a 2D form, getting so called vector files .*dxf* (fig. 14).
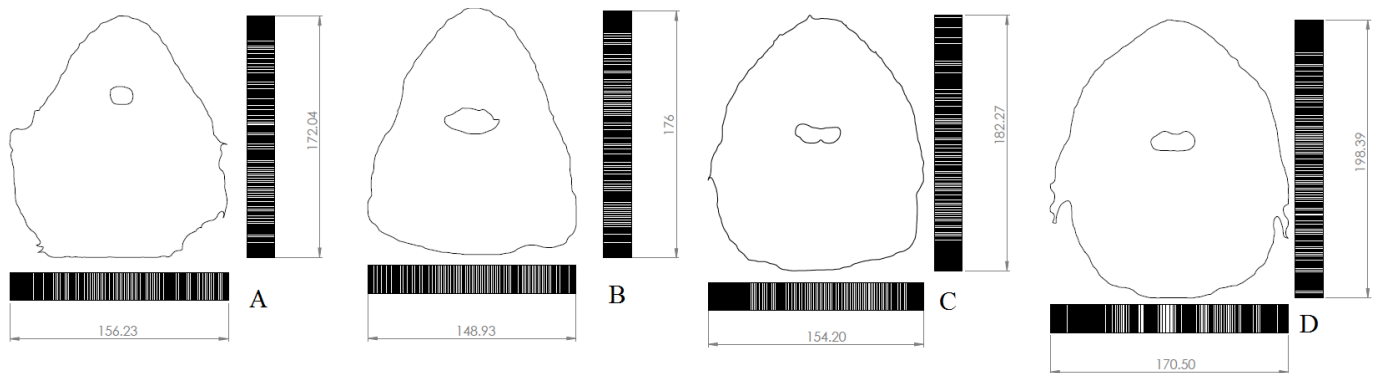
Figure 14. 2D form of slab phantom model

Recreating a real size phantom from a standard male patient 2D PMMA slabs has to be polished with a metal polisher recreating 3D form of the slab phantom (fig. 15 and fig. 16).
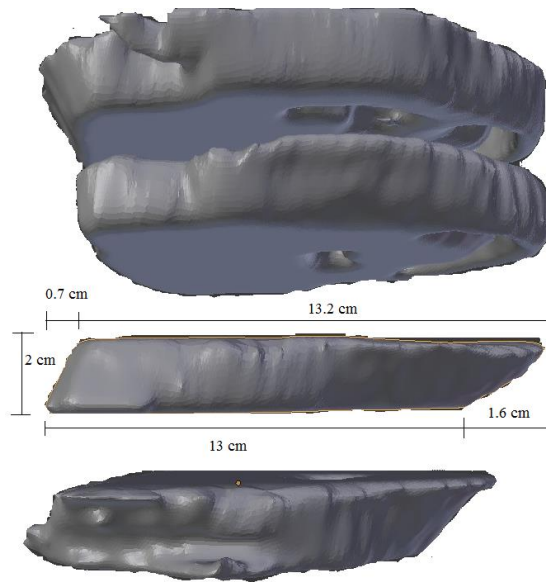
Figure 15. A model of the phantom in 3D

Figure 16. Result of polishing process; on the left – before polishing; on the right – after polishing

2.3 Irradiation dose registration using GAFchromic EBT2 films

The absorbed doses and doses distribution during irradiation procedure were determined using GAFchromic films EBT2. These GAFchromic films are self-developing and do not require any processing. The films are energy independent and are suited for the superficial radiotherapy experiments. It is easy manageable due to the stability in the room light and resistance to humidity and it is near tissue equivalency. The dose range is up to 10 Gy. These films have yellow dye which shows that it should be analysed using a red channel [50].

48 hours after irradiation the films were scanned with a scanner *HP Scanjet G400*. All the pieces of the films (cut-outs) should be scanned at the same orientation (the scanning light should be perpendicular to the scan direction), as manufacturer recommends. This removes the scanning artefacts and gives more accurate results (fig. 17) [50]. By following the manufacturer protocol the error of the measurement does not exceed 0.5%. [51]
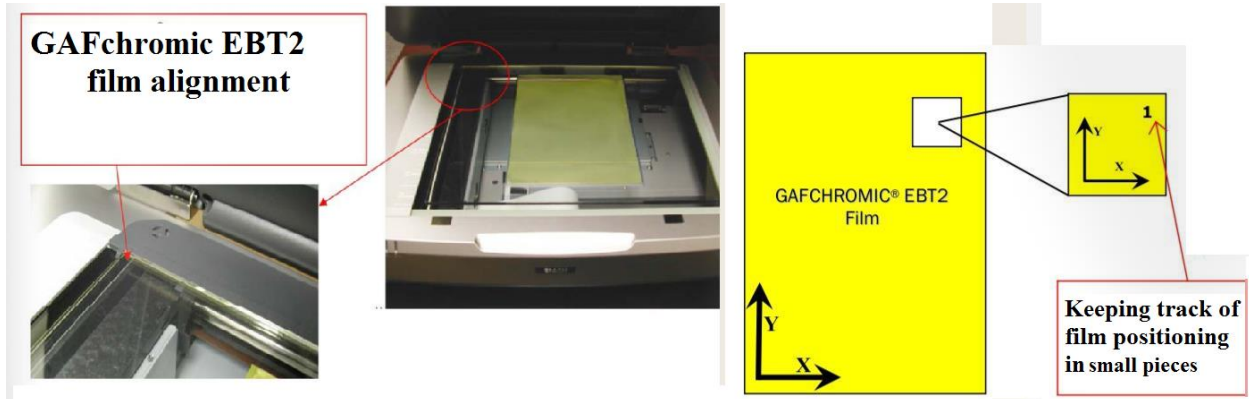

Figure 17. Film alignment in scanner and small piece track of film positioning [50]

Before the irradiation procedure and evaluation of absorbed doses and dose distributions GAFchromic films has to be calibrated. Pieces of the films ($2x2$ cm^2) irradiated in different doses, which differ from 0 Gy to 4.5 Gy (using 0.5 Gy step). Certain dose range was chosen, because for irradiation procedure was used 4 Gy/ fraction and one of task of this research was to evaluate the influence of the low doses to the OAR. The main parameters of irradiation procedure were: voltage – 80 kV; current – 20 mA; Focus to Skin Distnce (FSD) – 20 cm; applicator – A: 3 cm diameter; dose – 16 fractions, 4 Gy per fraction (461 MU), in total 64 Gy; depth – 0.5 cm, 2.44 mmAl.

The GAFchromic films were analysed depending on the manufacturer recommendations: the films were scanned after 48 hours after the irradiation process. The films get a darker colour depending on the dose delivered: the brightest film is the one, which was not irradiated and the darkest is the one irradiated with a dose of 4.5 Gy (fig. 18).
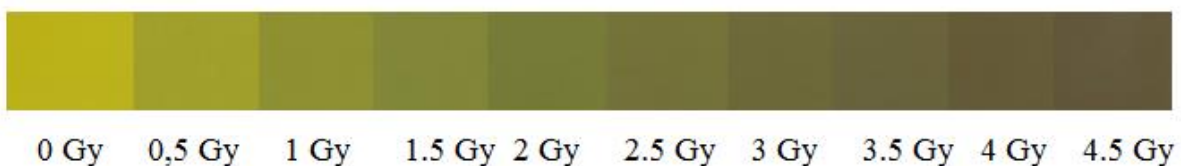
Figure 18. Scanned GAFchromic films after 48 hours from irradiation

The analysis of the GAFchromic films was made using a program *ImageJ*. The programme is designed to analyse scientific images and gives a detailed overview. It provides a lot of processing features and contains a toolbar of selections. *.bmp* or *.jpg* format file images can be analysed using channel of three colours – red, green or blue. A red component was chosen as recommended by the manufacturer (fig. 19). For the analysis the same size measurement area was chosen at each irradiated piece of the film. A calibration curve is drawn depending on the calculated results given in figure 20.
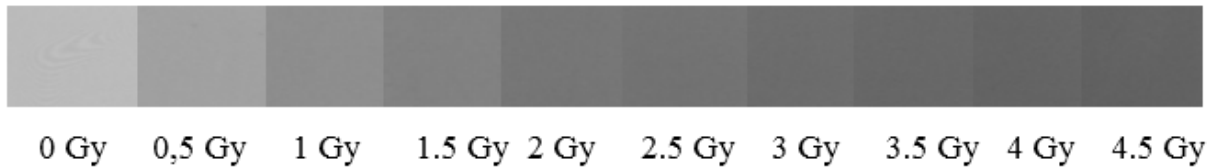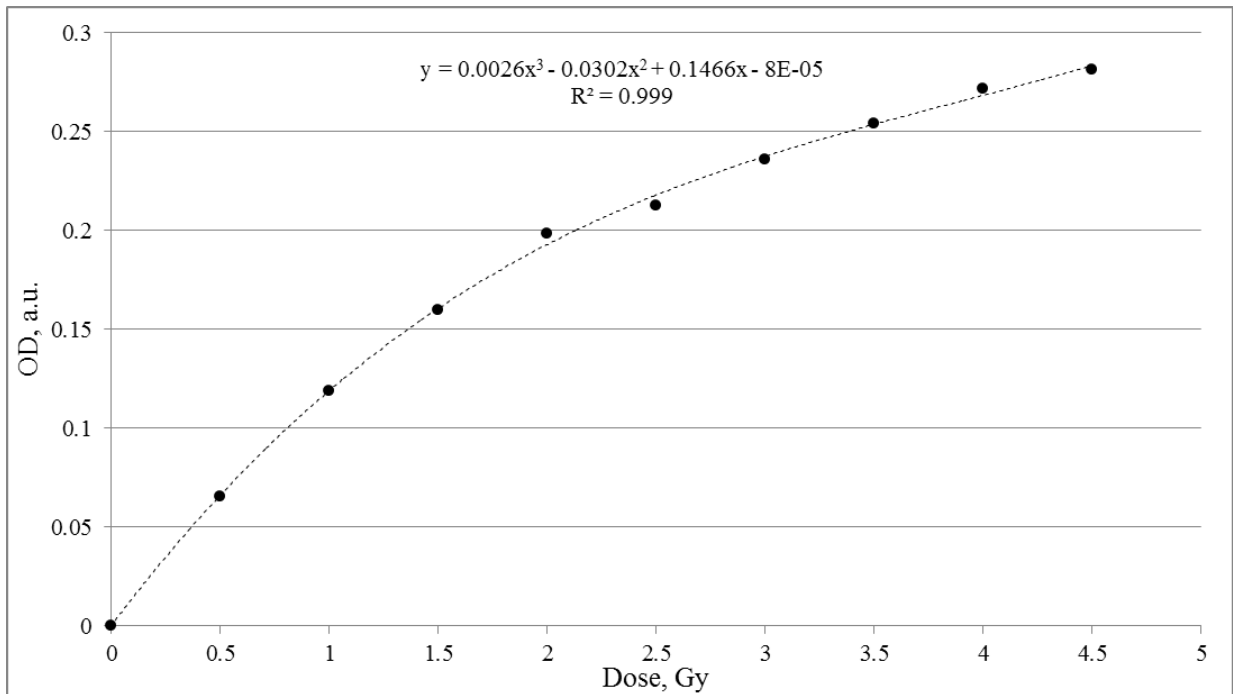

Figure 19. GAFchromic films with red component

Figure 20. Calibration curve of GAFchromic EBT2 films

The equation on the chart reads:

$$y = 0.0026x^3 - 0.0302x^2 + 0.1466x - 8\text{E-}05$$
$$R^2 = 0.999$$

For the greater accuracy the angular dependency of irradiation beam orientation was investigated and the irradiated films are evaluated (fig. 21).

Figure 21. GAFchromic film calibration process; A – film irradiated in a 90° angle, B – film irradiated at a 0° angle, C – film fragmentation for analysis with irradiation dose of 4 Gy, left – irradiated in condition A, right – in condition B

All the calibrated GAFcromic films for both calibration positions were analysed in small fragments of 2.8 mm to determine the change in colour intensity dependent on the angle. The results did not show any significant difference between the angle orientations to the irradiated film. It gives the ability to irradiate the GAFchromic films in any irradiation beam angular orientation to the film.

2.4 Irradiation process

Irradiation of the experimental setup was made using X-ray therapy unit GULMAY D3225. The X-ray unit GULMAY D3225 produce X-rays operating at the voltages in the $40 \div 220$ kV range, while maximum/peak energies is in the $40 \div 220$ kV range. It has several applicators (cones) that vary in diameters (irradiation field size) and lengths (focus skin/surface distance). This unit is suitable for superficial radiotherapy and orthovoltage X-ray therapy.

The parameters, which were chosen for the irradiation, are usually used for the superficial X-ray radiotherapy, treating bucca skin cancer patients' cases:

- Voltage – 80 kV;
- Current – 20 mA;
- Focus to Skin Distance (FSD) – 20 cm;
- Applicator – A: 3 cm diameter;

- Dose – 4 Gy per fraction (461 MU), 16 fractions, total 64 Gy;
- Depth – 0.5 cm.

The slab phantom was irradiated corresponding to bucca skin cancer patient case (right side), trying to keep applicator as close as possible to the phantom surface, and to use the same parameters of the irradiation as it is used in real patient case (figure 17). The experiment was made two times more, changing a position of the applicator angle ±2.5° (from the reference applicator angle position (102.5°)). Therefore each time the same region was irradiated using the same irradiation conditions, only making changes in the applicator positioning (fig 21).
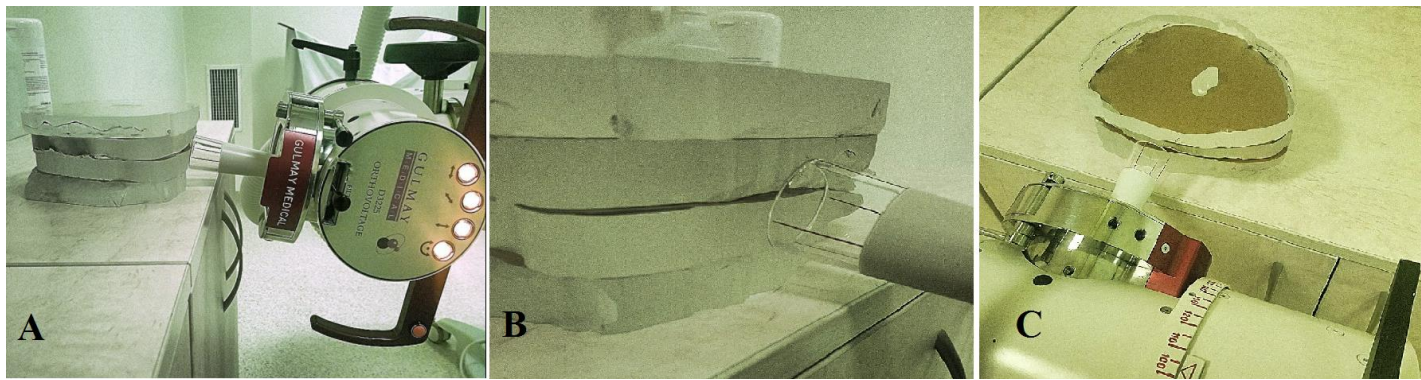

Figure 22. Positioning of the phantom: A – solid surface; B – applicator positioning; C – reference angle of 102.5°

Repetition of each procedure is always an intrigue issue in radiotherapy, especially positioning an orientation of the applicator. Applicator angle changes was chosen as a parameter of the irradiation procedure optimizing irradiation technique and preparing possible irradiation doses for critical organs registration methodology.
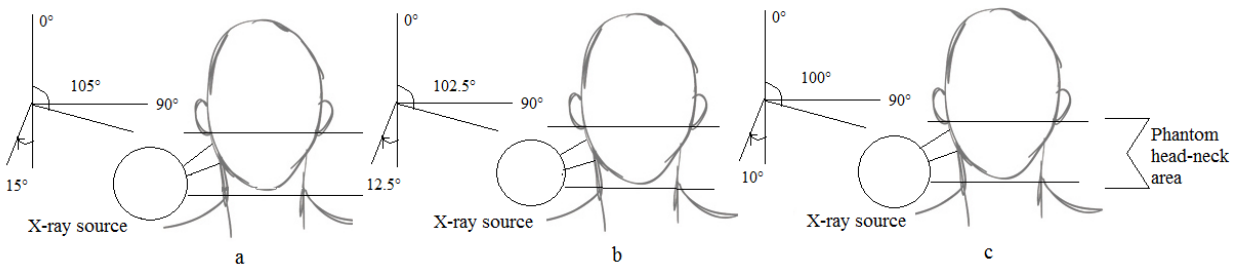
Figure 23. Experimental conditions; a - +2.5° from reference angle; b – reference angle; c - -2.5° from reference angle

2.5 Absorbed dose evaluation and dose spatial distribution

The plated slab PMMA phantom is made out of 4 different slabs (fig. 24). The pieces of GAFchromic EBT2 films were placed between the slabs.

Figure 24. Slab marking of plated phantom

After the irradiation procedure the irradiation beam paths are clearly seen on the films (fig. 25). The circles on each film show the localization of the critical organs. These regions are the main areas of interest, evaluating irradiation doses.

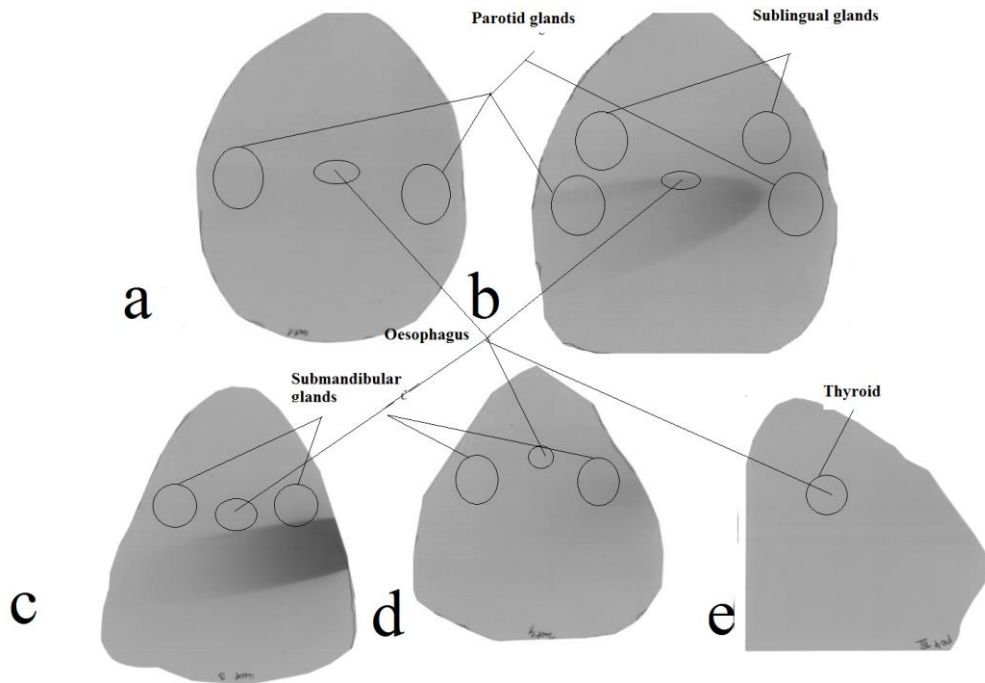Figure 25. Distribution of the dose in each GAFcromic film cut-out; a – on top of slab 1; b - between slabs 1 and 2; c – between slabs 2 and 3; d – between slabs 3 and 4; d – under slab 4

The letters (a, b, c, d and e) show the localization of the GAFchromic film between phantom slabs (fig. 26).
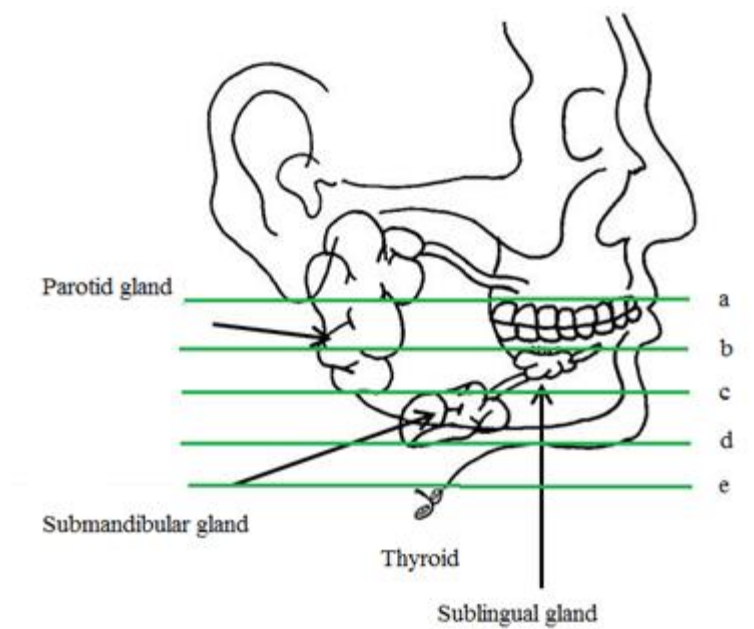

Figure 26. Localization of the GAFchromic films in the plated phantom and the position of the salivary glands

Some of the investigated critical due to size and location were evaluated into one or two films, for example, dose for parotid glands are evaluated into films a and b; submandibular glands b and c; sublingual glands being the smallest appears only in film b. Using the program *ImageJ*, was able to determine absorbed doses and their isodose distributions.

2.6 Effective dose evaluation

From the absorbed dose measurements of the critical organs (salivary glands, thyroid and oesophagus) the calculation of the effective dose can be done. To calculate the effective dose, the equivalent dose H_T should be determined which is dependent on various types of ionizing radiation weighing factors. The effective dose is then based on the biological effects. It is multiplied by a weighting factor W_R of ionizing radiation (2):

$$H_T = \Sigma \; W_R D_{T,R} \qquad (2)$$

SI unit - Sievert, 1 Sv = 1 J / kg.

The weighing factors of ionizing radiation could be seen in table 3.

Table 3. ICRP – 103 radiation weighing factors

Radiation type	Radiation weighing factor, W_R
Photons	1
Electrons, muons	1
Protons, charged pions	2
Alpha particles, heavy ions	20
Neutrons	Continuous function of energy

Table 3 describes the radiation weighing factors. A photon beam is used in the experiment so the dose can be recalculated using $W_R = 1$.

Effective radiation dose E - equivalent dose H_T, adjusted by taking into account human's organs or tissues sensitivity to ionizing radiation – multiplied by a weighting factor w_T (3)

$$E = \sum w_T H_T \qquad (3)$$

SI unit - Sievert, 1 Sv = 1 J / kg.

Tissue weighing factors could be observed in chapter 1.5 table 2, where the salivary glands have a tissue weighing factor of 0.01, thyroid and oesophagus of 0.04. By having all the measurement the effective dose can be depicted.

Lifetime Attributable Risk. It is known that tissue reactions depending on irradiation dose may occur from days to few weeks (early reactions) and/ or from months to years (late reactions). Possible time effect of reactions depends on cell type of tissues, proliferation rate, DNA repair and etc. The threshold of the irradiation dose depends on the type of injury and how injury is assessed. Also it is known that threshold of irradiation dose could be dependent for some normal tissues on the irradiated volume. In some cases, like spinal cord, radiation injury even to a small volume could be significant and could result in function disorder of the part or the whole organ.

Due to made ICRP recommendations radiation risk from the particular examinations is converted using nominal probability coefficients for the fatal cancer or radiation damage. There are presented international radiation risk models, like BEIR VII, UNSCEAR, ICRP, evaluating Lifetime Attributable Risk (LAR) of radiation induced cancer and fatal cancer as a function of effective dose [52-54]. It is known that BEIR VII Life Attribute Risk for all induced cancers is 0.012% per mSv, as for lethal all types of cancers are 0.006% per mSv; while accordingly ICRP: induced cancers – 0.017% per mSv; for mortality – 0.004% per mSv.

3. Results and discussion

The experimental measurements were made with the changing geometry (varying applicator angle position) of the irradiation procedure using the self-made prototype of PMMA slab phantom, which was recreated from the standard patient computed tomography (CT) images.

Irradiation of the slab phantom was made imitating the real skin cancer of buccal treatment procedure: 4 Gy/fraction (total of 64 Gy), voltage – 80 kV, current – 20 mA; focus to skin Distance (FSD) – 20 cm, applicator – A: 3 cm diameter, depth – 0.5 cm, reference tilt of the applicator angle was 102.5° (fig. 27)
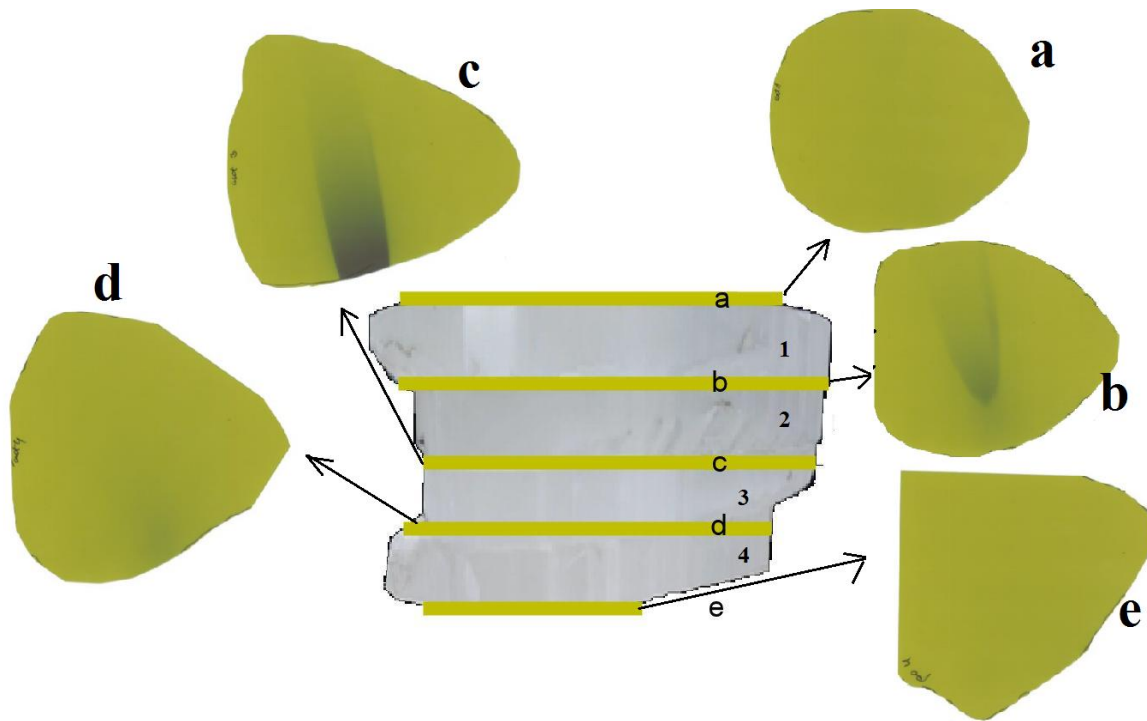
Figure 27. Slab phantom and film positioning

The head and neck region anatomically includes many OAR (fig. 28). The experiment gives the ability to evaluate the absorbed dose for each critical organ individually and determine the possible risks during the irradiation procedure. The figure 28 represents the OAR localisation in the head and neck area and can be determined in each film. The construction of the phantom gives the ability to place five GAFchromic EBT2 films, which represent a more accurate 2D distribution of the dose in each slice (between the slabs).

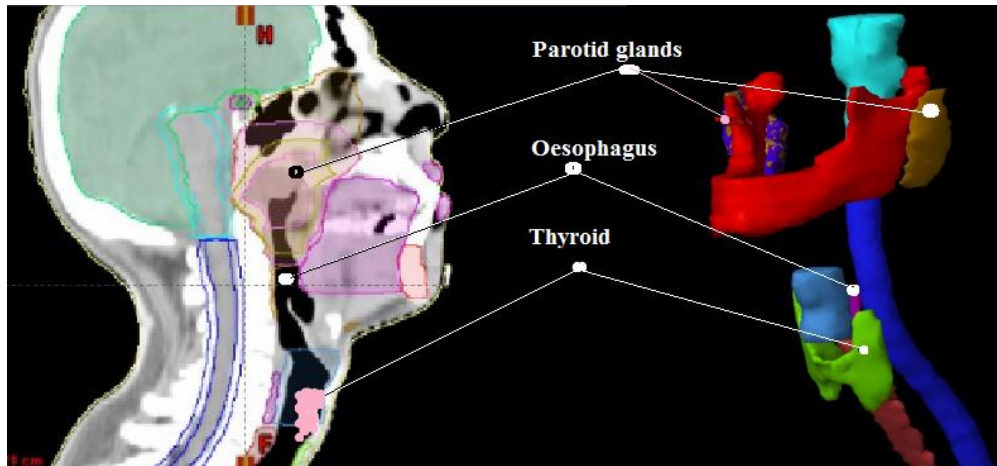Figure 28. The OAR in the slab phantom

Absorbed doses were measured using 2D GAFchromic films dosimetry. Film (c) is located in the direct pathway of the primary beam and shows the maximum dose of 4 Gy in ~5 mm from the phantom surface (fig. 27, fig. 28). So the attenuation process is the best seen in film (c) where the absorbed dose lowers from 4 Gy to 0.1 Gy (from 100 % to 2.5 %) across the irradiated phantom, i.e. irradiating the phantom from the right side to the left (fig. 30)

The results of measurements confirmed how important the beam angle position to the dose of the critical organs is. For example, the dose distribution of the absorbed dose (fig. 29), which shows the isodose distribution at a reference angle of 102.5°, clearly shows the main tendency of the dose scattering and attenuation processes into the volume depending on the applicator angle.
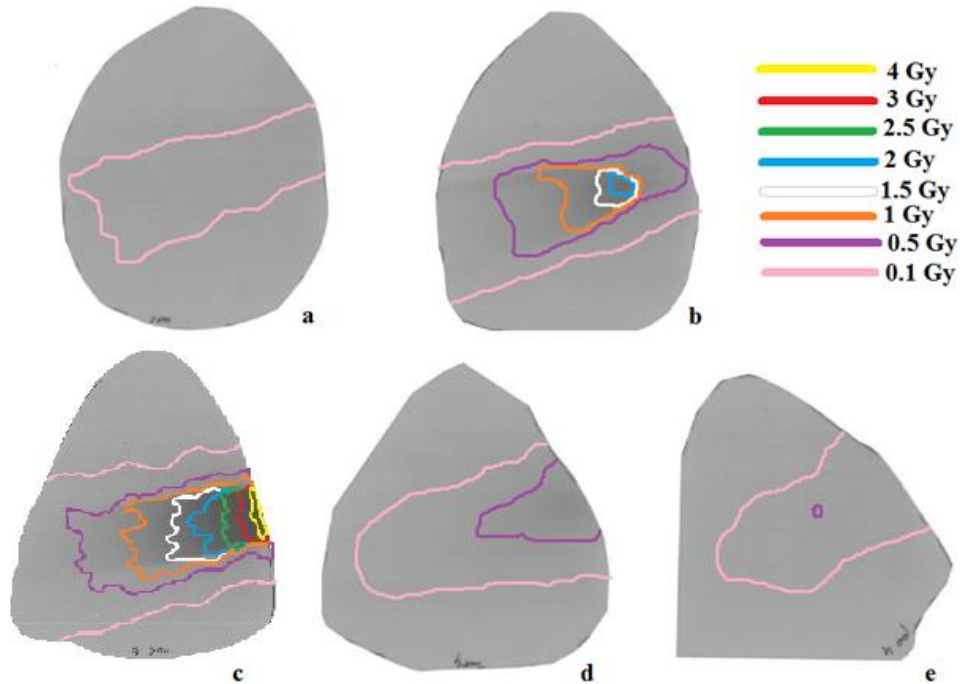
Figure 29. Dose distribution of GAFchromic EBT2 films in isodose curves
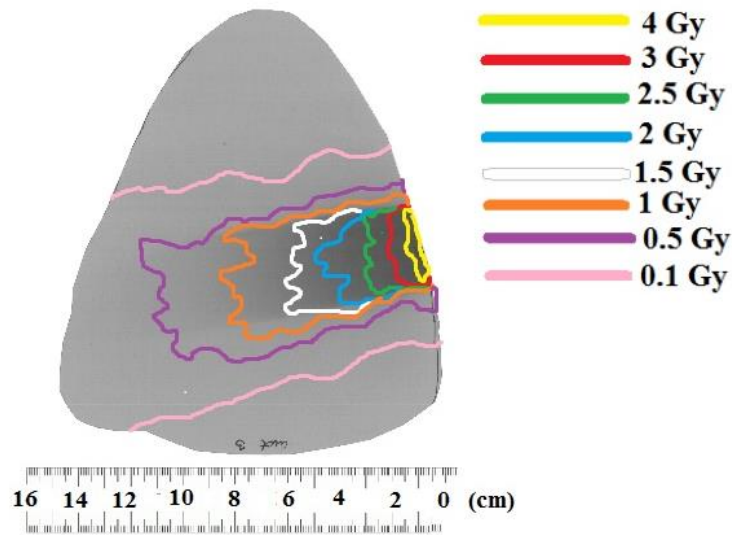
Figure 30. The attenuation in film (c)

The aim of the irradiation procedure was that the maximum prescribed dose was generated in 5mm depth. From the isodoses distribution of the measured absorbed doses in a slab phantom it is clearly seen that 100% of the prescribed dose is located in 5 mm depth and drops of rapidly in the deeper layers. In the depth of 8-9 cm only 25% of the maximum dose could be identified.

Due to measured absorbed doses evaluating angular dependency it is observed that the angle tilts of ±2.5° (fig. 31) from the reference angle could be significant depending on the tilt position towards the upper part of the head or towards the body. It is observed that depending on the location of the critical organs, for example the parotid glands, at the angle of 105° for the left and right parotid glands a tendency of dose lowering could be identified.
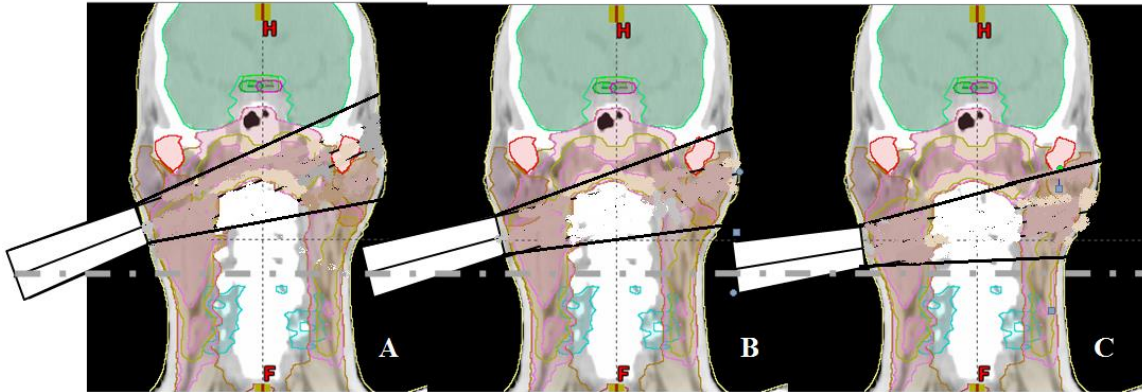

Figure 31. X-ray source positioning in different angles; A - 105°, B – 102.5° (reference angle), C - 100°

Table 4. Absorbed doses of the OAR

| Angle	Critical	Left side Absorbed, Gy	Right side Absorbed, Gy
102.5°	Parotid glands, upper part, film (a)	0.084	0.144
	Parotid glands, lower part, film (b)	0.081	0.558
	Sublingual glands	0.066	0.267
	Submandibular glands, upper part, film (c)	0.125	0.558
	Submandibular glands, lower part, film (d)	0.080	0.389
	Thyroid (middle)	0.107	
100°	Parotid glands, upper part, film (a)	0.044	0.186
	Parotid glands, lower part, film (b)	0.057	0.472
	Sublingual glands	0.079	0.220
	Submandibular glands, upper part, film (c)	0.091	0.698
	Submandibular glands, lower part, film (d)	0.072	0.508
	Thyroid (middle)	0.113	
105°	Parotid glands, upper part, film (a)	0.069	0.163
	Parotid glands, lower part, film (b)	0.036	0.300
	Sublingual glands	0.064	0.286
	Submandibular glands, upper part, film (c)	0.136	0.984
	Submandibular glands, lower part, film (d)	0.060	0.536
	Thyroid (middle)	0.122	
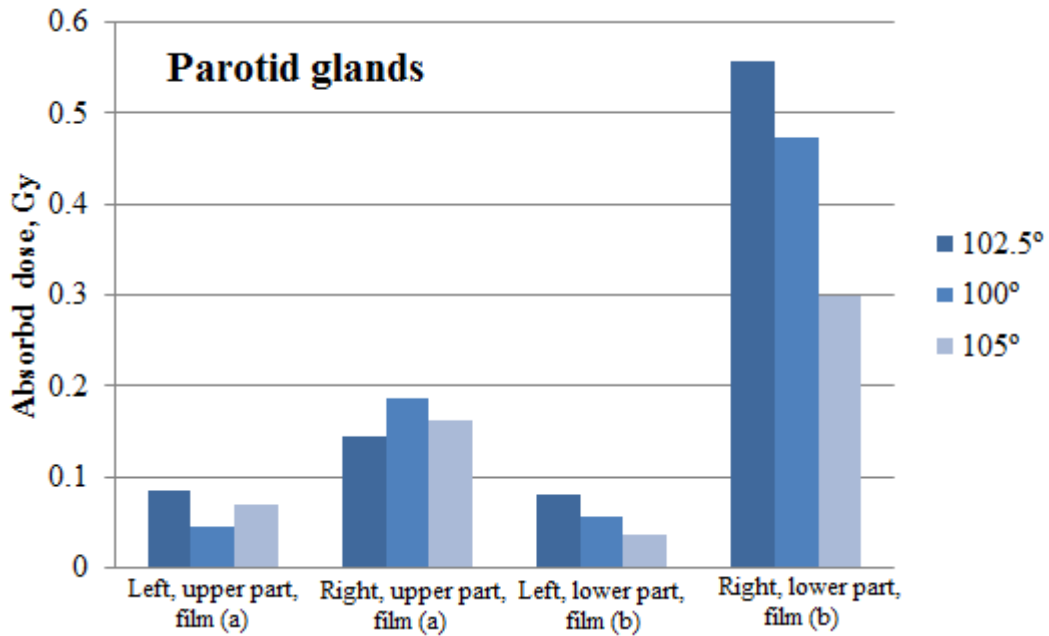
Figure 31. Absorbed to the parotid glands

In comparison with the absorbed doses of the parotid glands to submandibular right and left glands it is seen that a lower dose is received at the reference angle and the 100° than at the angle of 105° (fig. 32).
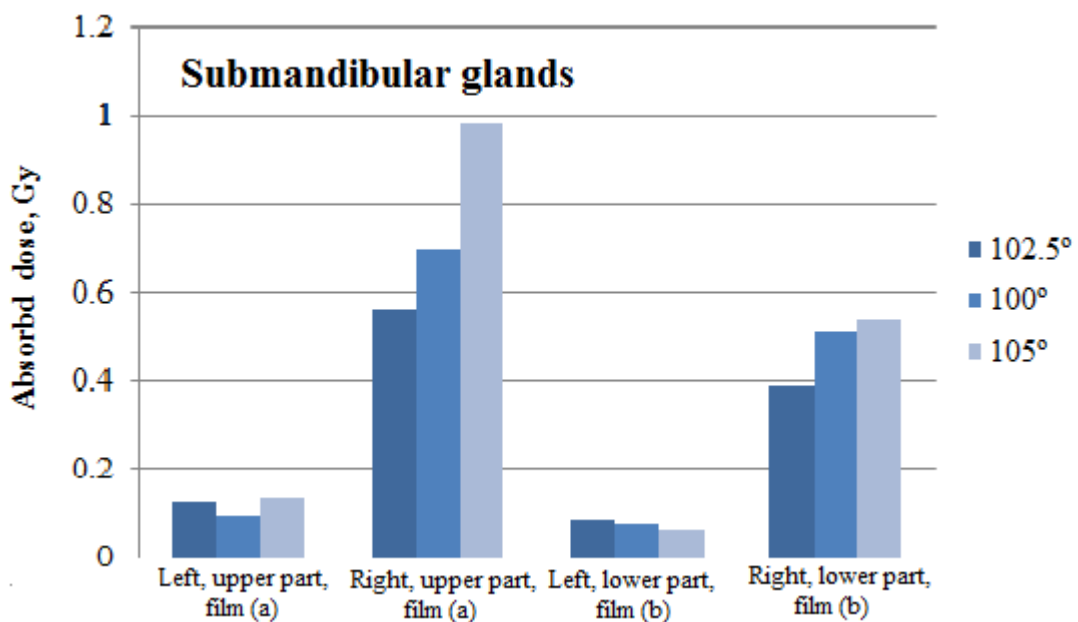
Figure 32. Absorbed dose to submandibular glands

In comparison with the right and left submandibular glands the same tendency could be identified in sublingual glands. The right and left glands receives a significantly higher dose at the tilted angle of 105º whereas the lower doses are delivered at angles of 100º and 102.5º (fig. 33).
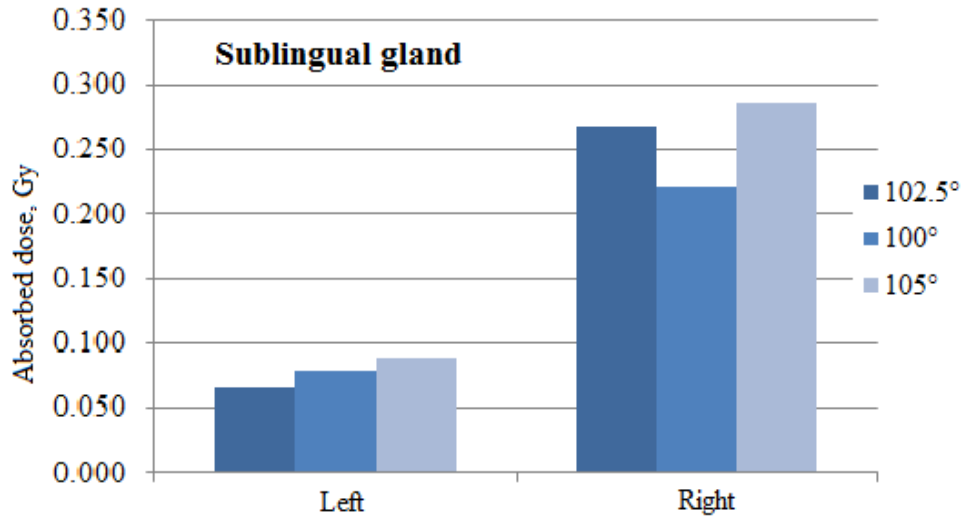
Figure 33. Absorbed dose to sublingual glands

While the salivary glands show a significant difference comparing the different irradiation angles the thyroid (film (e)) does not show similar tendencies. Comparing the irradiation angles the thyroid receives an absorbed dose that does not significantly differ. The irradiation angles were similar in all angles varying from.

Figure 34. Absorbed dose to thyroid

The positioning angle significantly changes the irradiation doses to the critical organs. The highest dose to the parotid glands is at the reference angle (18% and a 48% higher dose to the upper part and by 77% and 36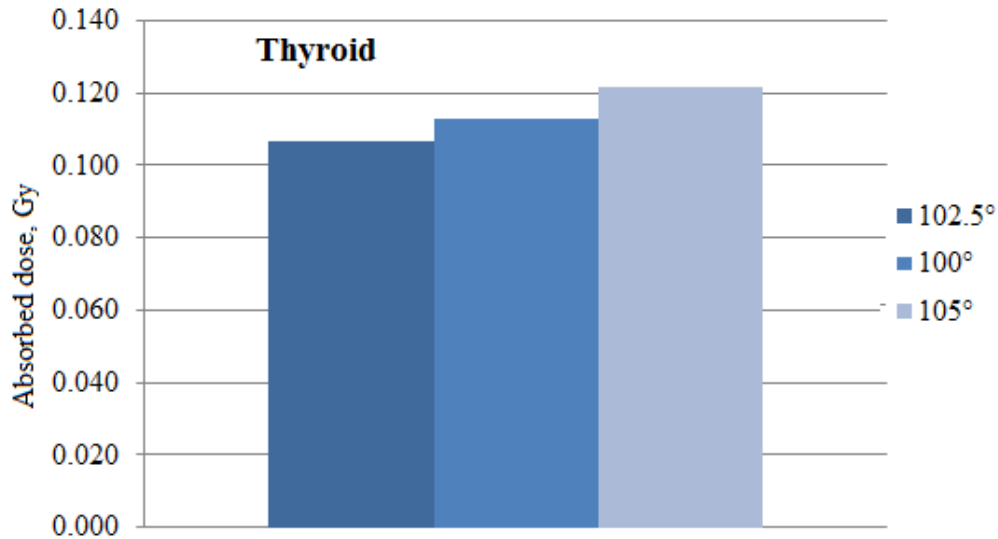% at the lower part than at angles of 105° and 100° respectively). However at the reference angle the doses are one of the lowest other critical organs submandibular (lower by 38.9% and 21.2% from the 105° and 100° respectively) and thyroid (by 5-12%). A similar tendency could be identified at the angle of 100º where the doses are in similar distribution as at a reference angle. At the angle of 105º an opposite tendency could be identified where the lowest dose is to the parotid glands and higher to submandibular, sublingual glands and thyroid.

3.1 Effective dose evaluation

Effective dose evaluation methodology usually is used in radiation protection to determine the general population irradiation (cancer risk in general) and is not applicable in radiotherapy field, due to the considerable inhomogeneity of the organs at risk (OAR). However, evaluating effective dose separately of each organ, it has a sense of effective dose methodology in radiotherapy (fig. 36). Accordingly to this, effective doses in radiotherapy usually are used as a lifetime risks for non-targeted critical organs, also it is known that calculation of effective doses mean a possibility to optimize the treatment procedure using lead shielding, changing geometry of the irradiation field and etc. [48]. Due to this reason preparing effective dose evaluation methodology as one of the criteria for the optimization of the irradiation procedure was to evaluate irradiation doses for the critical organs dependence on beam angle 100°, 102.5° (reference angle) and 105° (table 5).

Table 5. Effective doses to the OAR

| Angle	Critical	Left side Effective, mSv	Right side Effective, mSv
102.5°	Parotid glands, upper part, film (a)	0,840	1,443
	Parotid glands, lower part, film (b)	1,014	5,576
	Sublingual glands	0,657	2,673
	Submandibular glands,upper part, film (c)	1,253	5,576
	Submandibular glands, lower part, film (d)	0,803	3,888
	Thyroid (middle)	4,269	
100°	Parotid glands, upper part, film (a)	0,445	1,862
	Parotid glands, lower part, film (b)	0,566	4,724
	Sublingual glands	0,794	2,203
	Submandibular glands,upper part, film (c)	0,912	6,982
	Submandibular glands, lower part, film (d)	0,721	5,085
	Thyroid (middle)	4,514	
105°	Parotid glands, upper part, film (a)	0,694	1,629
	Parotid glands, lower part, film (b)	0,358	2,996
	Sublingual glands	0,637	2,862
	Submandibular glands,upper part, film (c)	1,364	9,838
	Submandibular glands, lower part, film (d)	0,597	5,356
	Thyroid (middle)	4,868	
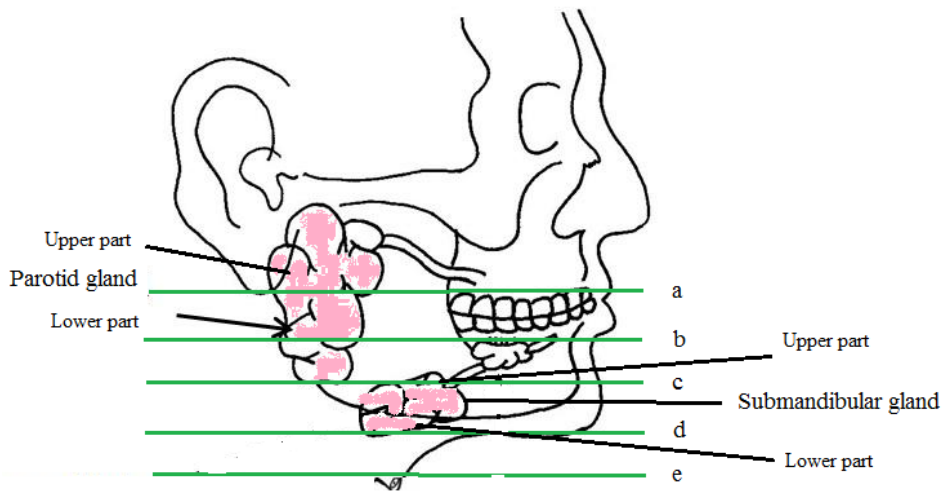
Figure 36. Upper and lower parts of parotid and submandibular glands

Irradiation beam angulated ±2.5° from the reference angle towards the head-neck area does not change the irradiation dose to the target but it changes the dose distribution in the critical organs.

Tilting the angle +2.5° from the reference angle (102.5°) the beam is directed towards the upper part of the head-neck phantom and it is registered that for the left side of the head-neck area irradiation doses are lower by at least 30% than to the right side. The right side of the phantom receives a similar dose from 1.4 to 9.8 mSv depending on the area in compare with the dose at the reference angle of the applicator (102.5°). Tilting the angle in the opposite side from the reference angle of applicator -2.5° the beam is directed to the neck side: the dose is lower to the parotid glands by at least 1.4 mSv (fig. 36 and 37), however submandibular and sublingual glands receive a higher dose by 0.3 mSv. The same tendency could be identified on the right side of the of the phantom with a lower dose to the parotid glands a higher dose to the sublingual (0.15 mSv) and submandibular glands.by 1.4-2 mSv

The effective doses distribution in compare to the different angles of the applicator on films (a) and (b) are shown in figure 36 for the parotid glands doses evaluation.

Effective doses registered on the film (a) and (b) for the right side parotid gland was 41.6% higher in compare with the left side parotid gland. The effective doses, due to size of the parotid glands were evaluated to the upper part (film (a)) and lower part (film (b)) of the parotid gland. Difference of the effective doses for upper (film (a)) and lower part (film (b)) of the right side (side of irradiation) parotid gland depending on the angle of the applicator was: 100° - 60.4 %, 102.5° - 74.1 %, and 105° - 43.5 %. These results showed that effective dose for the upper and lower part of the right side parotid gland the most significantly differs for the reference angle of the applicator. Almost the same tendency of the results was observed investigating the left side parotid gland with a higher dose to the upper part of the parotid glands at angles 100° - 20.9%, 102.5° - 16.8 %, and at the angle of 105° a lower dose of 49.8%

Evaluating the difference of the doses between the angles of the applicator for film (b) (lower part of parotid gland) for the angle 105° was registered 15.1% dose difference for the right side parotid gland in compare to the reference angle and 102.5° (fig. 32). For the film (a) accordingly to the results the difference between the angles not so significant (fig. 32), the maximum difference is between rotation of the angles 102.5° and 105° it is equal to 11.6%. The left side parotid gland at film (b) (lower part of parotid gland) significantly differ at 105° positioning angle with the dose being 76.9% lower comparing to the reference angle positioning.

For the film (a) accordingly to the results the difference between the angles is not so significant (fig. 38), the maximum difference is between rotation of the angles 102.5° and 100°

and it is equal to 29.1 %. The left side of the parotid gland in film (a) show a 48.6% higher dose at a reference angle. The same tendency could be determined in film (b) with the dose being 69.7% higher at the reference angle. The right side parotid gland in film (a) received a 22.6% higher dose at a tilted angle of 100° however in film (b) the dose was 15.6% higher at a reference angle.
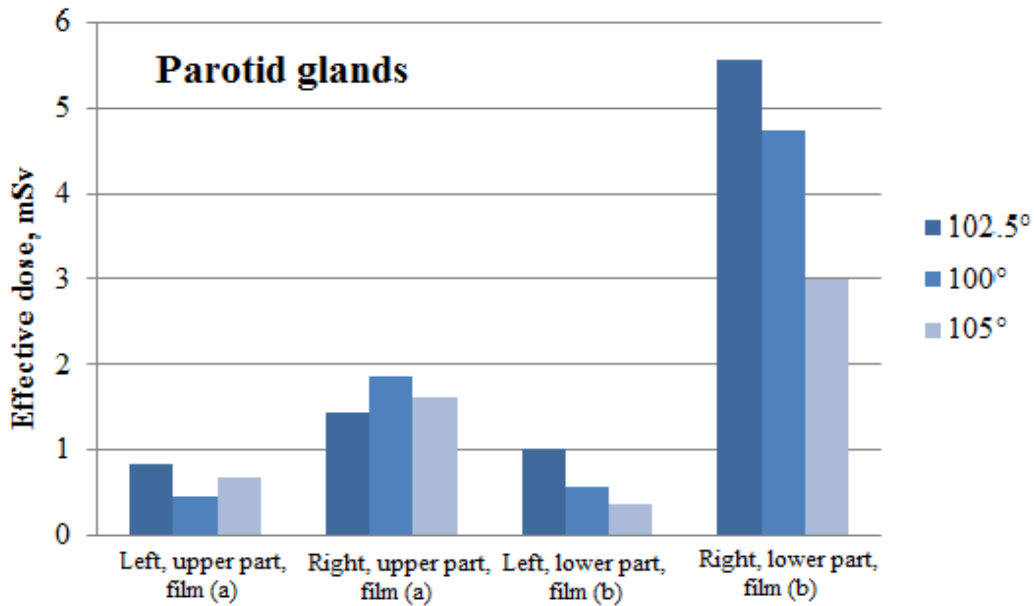
Figure 38. Effective dose to the parotid glands; film (a); film (b)

For the right and left parotid glands the lowest irradiation dose calculated rotating the angle 102.5° to 105°. For the left side of the submandibular glands there were not any significant changes registered but evaluating the left side of the glands. However comparing the right side of the glands the best choice would be the reference angle due to a significant difference at the lower part of the glands where the dose is lower by 30.78% and by 37.76% from the angles 100° and 105 respectively° (fig. 39).
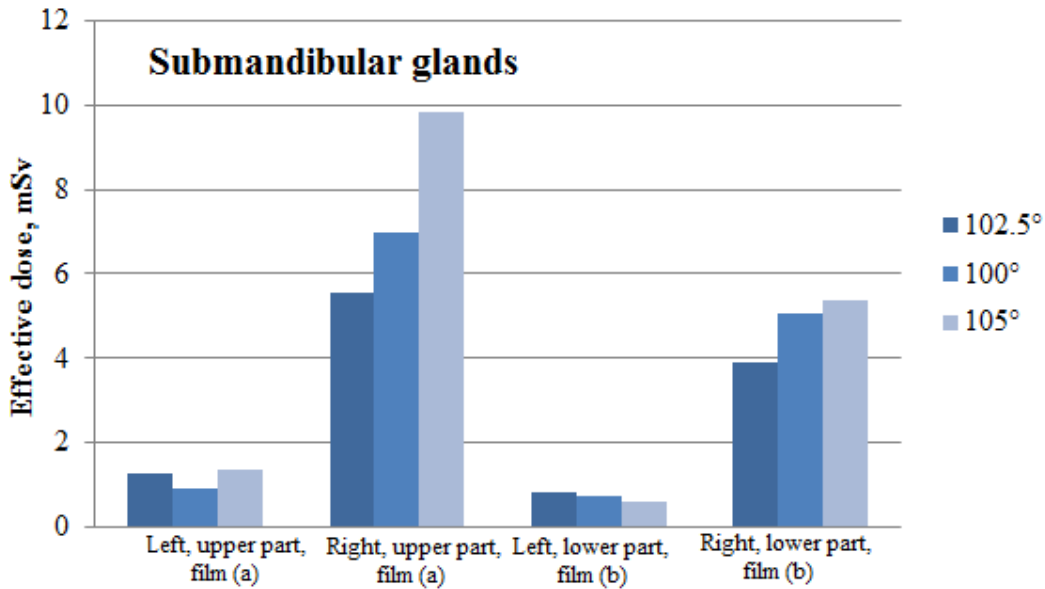
Figure 39. Effective dose to submandibular glands

A similar tendency could be observed evaluating the irradiation doses to the sublingual glands. The left side did not show any significant changes whereas the right side show the lowest dose received at the angle of 100°. At the reference angle a similar dose was received at reference angle and 105° angle (difference 7%). However the right sublingual gland receives a 17.58% lower dose at the tilted 100° angle from the reference angle (fig. 40)

Figure 40. Effective dose to sublingual glands

Thyroid gland is located at neck area is film (e). Although during the procedure the thyroid is not located at the direct beam path the effective dose could be identified at this area and the data is depicted in figure 41. It can be identified that the thyroid received the lowest effective 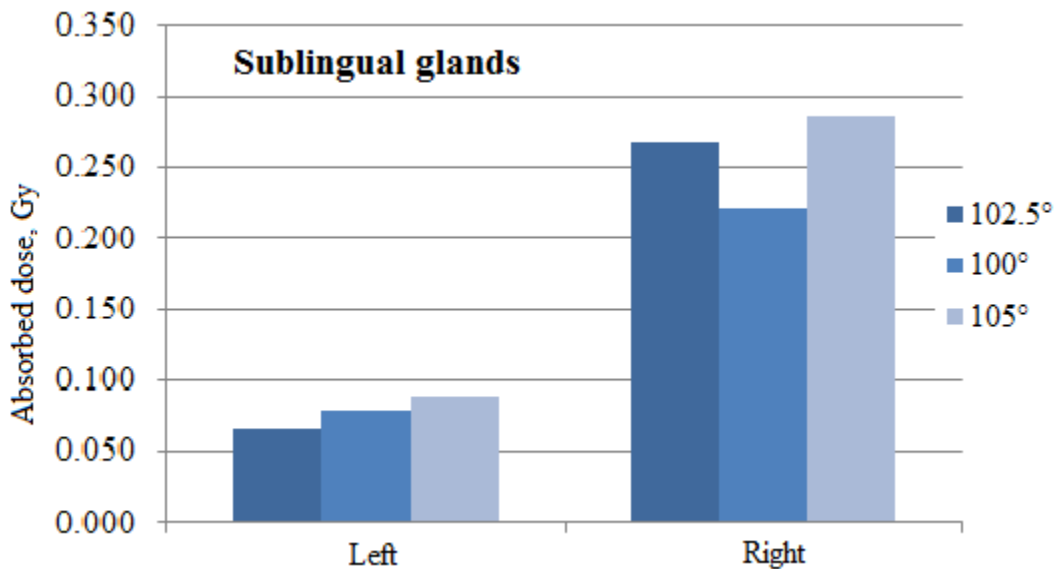dose at the reference angle of 102.5°. At the tilted angle of +2.5° the effective dose is 14.03% higher comparing to the dose delivered at the reference angle. At the tilted angle of -2.5° the dose differs from the reference angle by 5.74%.
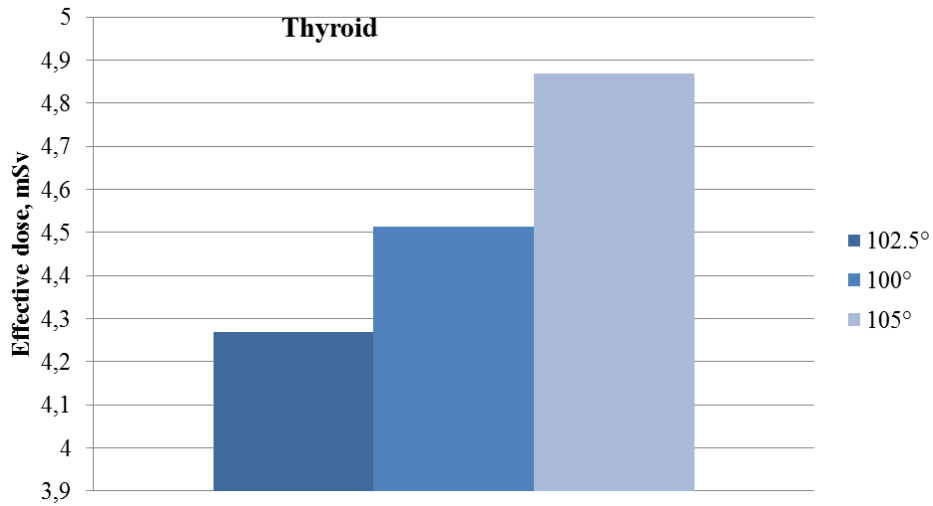
Figure 41. Effective dose to thyroid

Lifetime Attributable Risk evaluation as a function of the mean effective dose, for the irradiation procedure, imitating buccal skin cancer patient treatment, during whole treatment process for the different angular dependencies estimating dose to risk conversation factor for induced cancer and for mortality accordingly to BEIR VII (LAR for all induced cancers is 0.012% per mSv, lethal all types of cancers are 0.006% per mSv) is depicted in table 7.

Table 6. Lifetime attribute risk

Rotation angle	Induced secondary cancer per 100 000 individuals	Mortality per 100 000 individuals
100º	3.7	1.9
102.5º	3.5	1.8
105º	4.0	2.0

Conclusions

1. A prototype of the slab PMMA phantom was created using real standard male patient's CT images, imitating location of the critical organs, like parotid glands, submandibular glands, sublingual glands, thyroid and oesophagus. 2D films dosimetry was used for evaluation of irradiation doses for the critical organs depending on an angle of the applicator (100°, 102.5° and 105°) and optimizing the procedure of irradiation in superficial radiotherapy for the bucca skin cancer patient.

2. The absorbed dose measurements and dose distribution evaluation results showed significant difference on irradiation doses to the critical organs depending on an angle of the irradiation beam. Measurements performed at the angle 105º showed a tendency of growing dose for the critical organs located in an upper part of the phantom, e.g., to the right submandibular gland dose at upper part was higher 76.43% in compare with the lower part of the gland. Changing the angle to 100º led to increased doses of the upper part of right submandibular gland by 30.78% higher absorbed dose than the lower part of the gland.

   Recalculation of the effective doses for each organ at risk and especially for non-targeted organs allowed evaluation of a mean lifetime risk induced by irradiation. It was shown that irradiation beam rotation by ±2.5° from the reference angle have a significant impact on the increased risk of radiation induced secondary cancer.

3. It was shown that the angle rotation of the irradiation beam during superficial radiotherapy treatment of buccal skin and may lead to the optimization of radiation procedure and reduction of doses to organs at risk. It is especially important in the case of the radiosensitive right side parotid gland since it is known, that the highest level of apoptosis in parotid glands is observed already at 24 hours after the 2 Gy irradiation procedure.

Literature

1. G. K. SVENSSON, CHAIRMAN. Physical Aspects Of Quality Assurance In Radiation Therapy Aapm Report No. 13. In: American Association Of Physicists In Medicine By The American Institute Of Physics, 1994.

2. A. D. WRIXON. Review New ICRP Recommendations. In: Journal Of Radiological Protection Prot. 28, 2008, pp 161–168.

3. J. P. GLEES, V WOLSTENHOLME. The Role of Kilovoltage X-rays in the Treatment of Skin Cancers. European Oncological Disease, 2006, pp. 32-37 Cancer of the Skin

4. L. MARGOLIS. Leibel and Phillips Textbook of Radiation Oncology (Third Edition), 2010

5. M. ALLEN CHEN. Evaluation of depth dose characteristics of superficial X-rays machine using different KVP and applicators diameter. Iranian journal of radiation research, 2011, pp. 159-166.

6. K. RYAN, FUNK, N. NADIA, I. LAACK. Basics of Radiation Therapy. Clinical Cardio-Oncology, 2016, pp. 66-73

7. S. MCGREGOR, D. PHARMD, J. MINN, D. FAO, D. HEROLD. "Superficial Radiation Therapy For The Treatment Of Nonmelanoma Skin Cancers. In: The Journal Of Clinical And Aesthetic Dermatology, 2015, pp. 12–14.

8. G. ANAND. Review on the characteristics of radiation detectors for dosimetry and imaging. Physics in Medicine and Biology, 2013, pp. 303–347.

11. The 2007 Recommendations Of The International Commission On Radiological Protection. Annals Of The Icrp. Icrp Publication 103. 37 (2–4).

10. S. GALLIK. HistologyOLM, The On-Line Laboratory Manual For Mammalian Histology, *Hystology OLM,* 2013.

12. S. K. GILL, A. NIROLA, A. P. MAINI, R. SIDHU, "Radiation Induced Salivary Gland Damage: Review On Pathogenesis And Management". In: Journal Of Dental Sciences, 2016

13. G. C. JAGUAR, J. D. PRADO, D. CAMPANHÃ, FÁBIO A. ALVES. Clinical Features And Preventive Therapies Of Radiation-Induced Xerostomia In Head And Neck Cancer Patient: A Literature Review. In: Applied Cancer Research, 2017, pp. 31-37.

14. E. YODEN, T. SOEJIMA, T. MARUTA, Y. DEMIZU, H. NISHIMURA, Y. EJIMA, R. SASAKI, K. YAMADA. Hypothyroidism After Radiotherapy To The Neck. In: Danish Medical Journal, 2004, pp. 146-50.

15. Hygiene Standard HN 73:2001 "Basic Standard Of Radiation Protection". Adopted By The Order No. 663 On 21 December 2001 By The Minister Of Health Care of LR.

16. Hygiene Standard HN 95:2005 "Radiation Protection and Quality Control in radiotherapy" Adopted by the Order No. V-759 of 10 October 2005 by the Minister of Health Care.

17. R. HILL, B. HEALY, L. HOLLOWA, Z. KUNCI, D. THWAITEs, D. BALDOCK. Advances In Kilovoltage X-Ray Beam Dosimetry. In: Physics In Medicine And Biology, 2014, 59-65.

18. D.I. THWAITES, B.J. MIJNHEER, J.A. MILLS; Chapter 12. Quality Assurance Of External Beam Radiotherapy. IAEA.Org - Seen 2018.03-25

19. Absorbed Dose Determination In External Beam Radiotherapy An International Code Of Practice For Dosimetry Based On Standards Of Absorbed Dose To Water. Technical Reports Series No. 398, Iaea Vienna, 2000

20. International Commission On Radiation Units And Measurements. Report 76: Measurement Quality Assurance For Ionizing Radiation Dosimetry. Journal Of The ICRU 1–3, 2006.

21. J. Harrison. Use of Effective Dose. 3rd International Symposium on the System of Radiological Protection, 2015, Seoul.

22. C. D. JOHNSTONE, R. LAFONTAINE, Y. POIRIER, "Tabasco Modeling A Superficial Radiotherapy X-Ray Source For Relative Dose Calculations"; Journal Of Applied Clinical Medical Physics, Volume 16, Number 3, 2015

23. POIRIER Y, KOUZNETSOV A, KOGER B, TAMBASCO M. "Experimental Validation Of Kilovoltage X-Ray Source Model For Computing Imaging Dose". Med Phys. 2014

24. K. MCMILLAN, M. MCNITT-GRAY, D. RUAN. Development And Validation Of A Measurement-Based Source Model For Kilovoltage Cone-Beam Ct Monte Carlo Dosimetry Simulations. In: Medical Physics, 2013.

25. ICRP Statement on tissue reactions and early and late effects of radiation in normal tissues and organs — threshold doses for tissue reactions in a radiation protection context. ICRP Publication 118. Ann ICRP 2012.

26. N. Hamada, and Y. Fujimichi Classification of radiation effects for dose limitation purposes: history, current situation and future prospects. ICRP Journal of Radiation Research, 2014, pp. 629–640.

27. A. D. WRIXON CASTELLEZGASSE. Review New Icrp Recommendations 25/2/6, 1020. Vienna, Austria, 2008

28. Recommendations of the International Commission on Radiological Protection. ICRP Publication 26. Ann ICRP 1977.

29. J. GUO, D. ZHAO *et. al*. Protective Effects of Hydrogen against Low-Dose Long-Term Radiation-Induced Damage to the Behavioral Performances, Hematopoietic System, Genital System, and Splenic Lymphocytes in Mice. *Oxidative Medicine and Cellular Longevity*, 2016, pp. 1-15.

30. R. LALL, S. GANAPATHY , M . YANG, S. XIAO, T. XU, H SU, SHADFAN M, J. M. ASARA JM, , BEN-SAHRA, B. D. MANNING, LITTLE JB, YUAN ZM. Low-dose radiation exposure induces a HIF-1-mediated adaptive and protective metabolic response. Cell death and differentiation, 2014, pp. 836-844.

31. H. MENZEL. ICRP Symposium On The International System Of Radiological Protection. 2011 – Bethesda, Md, Usa, 2011

32. ICRP Publication 103. ICRP Publication Ann. ICRP 37. 2007.

33. A. K. BAKSHI. Energy Response Study Of Thermoluminescense Dosimeters To Synchrotron Radiation Energy Range 10-5 Kev. In: Indian Journal Of Engineering And Material Sciences, Vol 26, 2009, pp. 172-174.

34. M. BOUTILLON, A. M. PEROCHE. Ionometric Determination Of Absorbed Dose To Water For 60co Gamma Rays". In: Physics in Medicine & Biology, 1993, pp. 439–454.

35. NE Technology. Service Manual For Rialto. Beenham : Ne-Press, 1992.

36. M. ZELIKMAN, S. KRUCHININ, E. ISAYCHEVA. Calibration Of Thermoluminescent Dosimeters Placed Inside The Anthropomorphic Phantom Which Is Used For Ct Effective Dose Evaluation. In: European Society Of Radiology, 2012, 123-133.

37. S. C. SELVAMUTHUKUMAR, S. U. NISA, V. K. PARTHASARATHY, M. A. SAHABUDEEN, R. PAMULA, N. R. SIDDAREDDY. Estimation Of The Annual Cumulative Radiation Dose Received By The Dentist In Dental Clinics In Chennai. In: Journal Of Indian Academy Of Ral Medicine And Radiology, 2014, pp. 24-29,

38. S. PAUKŠTYTĖ, B. G. URBONAVIČIUS. TLD Dose Response To Different Radiotherapy Beam Qualities. In: Medical Physics In The Baltic States, 2017, pp. 89-93

39. A. Y. ABADI, A. A. MOWLAVI, R. I. N. ABADI, M. GHORBANI. Calculation And Comparison Of Md-55-2 And Hs Radiochromic Films' Responses To The 60co Gamma Rays. In: Archive Of Oncology, 2012, pp. 156-168.

40. W. L. MCLAUGHLIN, A. S. MEIGOONI, R. NATH, J. E. RODGERS, C. G. SOARES. Radiochromic film dosimetry: Recommendations of AAPM Radiation Therapy Committee Task Group 55. *American Association of Physicists in Medicine,* 1998, pp. 2093-2115.

41. A. NIROOMAND-RAD, C. R. BLACKWELL, B. M. COURSEY K. P. GALL, CHRISTOPHER. Radiochromic Film Dosimetry. In: Medical Physics, Vol. 25, Issue 11, 1998.

42. R., WILLIAM. Visible And Ultraviolet Spectroscopy. Retrieved 2014-10-29.

43. www.iba-dosimetry.com – seen 2018-03-30

44. ICRP Publication 103 Ann. ICRP 37 (2-4), 2007

45. H. YOSHITOMI, M. KOWATARI. Influence Of Different Types Of Phantoms On The Calibration Of Dosemeters For Eye Lens Dosimetry. In: Radiation Protection Dosimetry, 2016, pp. 199–203.

46. V. GIACOMETTI A, S. GUATELLI A,⇑, M. BAZALOVA-CARTER B, A.B. ROSENFELD A, R.W. SCHULTE. Development Of A High Resolution Voxelised Head Phantom For Medical Physics Applications. In: Physica Medica, 2017.

47. A. CHRISt, W. KAINZ, E. G. HAHN, K. HONEGGE, M. ZEFFERE, E. NEUFELD, W. RASCHER, R. JANKA, W. BAUTZ, J. CHEN, B. KIEFER, P. SCHMITT, H. HOLLENBACH, J. SHEN, M. OBERLE, D. SZCZERBA, A. KAM, J. W. GUAG, And N. KUSTER. The Virtual Family Development Of Surface Based Anatomical Models Of Two Adults And Two Children For Dosimetric Simulations. Physics in Medicine & Biology, 2010, pp. 23–38.

48. C. GRANLUND. Absorbed Organ And Effective Doses From Digital Intra-Oral And Panoramic Radiography Applying The Icrp 103 Recommendations For Effective Dose Estimations. In: The British Institute Of Radiology, 2016.

49. M. HEMANTH, M. VIDYA, NANDAPRASAD, V. BHAVANA, KARKERA. Sex determination using dental tissue. Medico-Legal Update, 2008, pp. 2-8.

50.*GAFchromic EBT2 Scan Handling Guide,* Advanced Materials, ISP, 2009.

51. D. Lewis, A. Micke, X. Yu. An efficient protocol for radiochromic film dosimetry combining

calibration and measurement in a single scan. *Journal of Applied Clinical Medical Physics,* 2012, pp. 6339 – 6350.

52. *UNSCEAR. Effects of ionizing radiation-Volume I: Report to the General Assembly, Scientific Annexes A and B.* UNSCEAR 2006

53. *Scientific Committee on the Effects of Atomic Radiation. United Nations sales publication E.08.IX.6.* United Nations, New York, 2008.; ICRP.

54. The 2007 Recommendations of the International Commission on Radiological Protection. ICRP Publication 103. Ann. ICRP 37(2-4), 2007.